

PEOPLE'S DEMOCRATIC REPUBLIC OF ALGERIA  
Ministry of Higher Education and Scientific Research  
National Polytechnic School



المدرسة الوطنية المتعددة التقنيات  
Ecole Nationale Polytechnique

Department of Metallurgy  
Dissertation Presented for obtaining the degree of State Engineer in  
Materials Engineering

**A diffusion-based simulation for the degradation of  
magnesium-zinc biodegradable orthopedic implants**

REZZIK EL MARHOUN Oussama, RIAHI Nouredine

Under the direction of : Mr M.CHITROUB Pr (ENP)

Presented and defended on: 27/09/2020

**Composition of the Committee:**

President	Mr A. KASSER	LCA (ENP)
Advisor	Mr M. CHITROUB	Pr (ENP)
Examiner	Mr A. DAIMELLAH	Dr (ENP)
Examiner	Mr M.LARIBI	Pr (ENP)



PEOPLE'S DEMOCRATIC REPUBLIC OF ALGERIA  
Ministry of Higher Education and Scientific Research  
National Polytechnic School



المدرسة الوطنية المتعددة التقنيات  
Ecole Nationale Polytechnique

Department of Metallurgy  
Dissertation Presented for obtaining the degree of State Engineer in  
Materials Engineering

**A diffusion-based simulation for the degradation of  
magnesium-zinc biodegradable orthopedic implants**

REZZIK EL MARHOUN Oussama, RIAHI Nouredine

Under the direction of : Mr M.CHITROUB Pr (ENP)

Presented and defended on: 27/09/2020

**Composition of the Committee:**

President	Mr A. KASSER	LCA (ENP)
Advisor	Mr M. CHITROUB	Pr (ENP)
Examiner	Mr A. DAIMELLAH	Dr (ENP)
Examiner	Mr M.LARIBI	Pr (ENP)

You should enjoy the little detours to the fullest. Because that's where  
you'll find the things more important than what you want.

— Yoshihiro Togashi

## DEDICATION

I dedicate my dissertation work to my family and many friends. A special feeling of gratitude to my loving parents, who I owe everything and to my big brother Moncef.

I also dedicate this dissertation to my many friends who have supported me throughout the years. I will always appreciate all they have done, especially Tinders, Pledge of The Friends, and my dear friend Oussama.

— Oussama

## DEDICATION

I dedicate my thesis work with very profound gratitude to my parents and to my siblings for providing me with unfailing support and continuous encouragement throughout my years of study and through the process of researching and writing this thesis. This accomplishment would not have been possible without them. They were always there for me and I hope one day I can repay at least a little bit from what they gave me.

My profound gratitude and love

Noureddine

## ACKNOWLEDGEMENTS

Foremost, we would like to express my sincere gratitude to our supervisor Professor Mohamed CHITROUB for the continuous support of our thesis study and research, for his patience, motivation, enthusiasm, and immense knowledge. His guidance helped us in all the time of research and writing of this thesis. We could not have imagined having a better supervisor and mentor for our master thesis study.

Besides our supervisor, I would like to thank the rest of our thesis committee: Dr A.KASSER, Dr A.DAIMELLAH, and Professor M.LARIBI for their encouragement and insightful comments.

Finally I would like to thank all teachers in our school department that helped us throughout the years.

## ملخص:

نظرًا لأنه قابل للتحلل البيولوجي وموصل للعظام، يوفر المغنيسيوم بديلاً واعدًا لمواد زرع العظام التقليدية. يتمتع المغنيسيوم بالخصائص الميكانيكية اللازمة لدعم الأنسجة الأساسية أثناء التعافي، مثل الكثير من مواد زرع العظام التقليدية يتآكل المغنيسيوم وتسمح خصائصه الناقلة للعظم باستبداله بالعظام الأصلية عند إدخاله في الجسم، مما يلغي الحاجة إلى إجراء عمليات جراحية أخرى لاستخراج المقومات المزروعة بعد الشفاء. تم تنفيذ وتشغيل محاكاة في برنامج "COMSOL Multiphysics"، قمنا بمحاكاة مقوم عظم فخذ من المغنيسيوم والزنك في ظروف مشابهة لتلك الموجودة في جسم الإنسان ثم ناقشنا المعطيات المتحصل عليها.

**الكلمات الرئيسية:** قابلة للتحلل البيولوجي، المغنيسيوم، الزنك، محاكاة، كمسول متعدد الفيزياء، تقويم العظام.

## Résumé:

Comme il est à la fois biodégradable et ostéoconducteur, le magnésium constitue une alternative prometteuse aux matériaux d'implants orthopédiques conventionnels. Le magnésium a les propriétés mécaniques nécessaires pour soutenir le tissu sous-jacent pendant sa guérison, tout comme les implants conventionnels. Lorsqu'il est inséré dans le corps, le magnésium se corrode et ses propriétés ostéoconductrices lui permettent d'être remplacé par des os natifs, éliminant ainsi la nécessité d'une intervention chirurgicale supplémentaire. L'étude de modélisation se fait sous Solidworks et Comsol, nous avons simulé l'alliage Mg-Zn dans des conditions similaires à celles du corps humain puis on a discuté des données obtenues.

**Mots-clés:** biodégradable, Magnésium, Zinc, simulation, Comsol, orthopédique, implant

## Abstract:

As it is both biodegradable and osteoconductive, magnesium provides a promising alternative to conventional orthopedic implant materials. Magnesium has the mechanical properties required to sustain the underlying tissue as it heals, much like conventional implants. When inserted in the body, magnesium corrodes and its osteoconductive properties allow it to be replaced by native bones, removing the need for further surgery. The modeling and simulation is done by COMSOL Multiphysics software, we simulated Mg-Zn alloys under conditions similar to those in human body and then we discussed the obtained data.

**Keywords:** biodegradable, Magnesium, Zinc, simulation, COMSOL Multiphysics, orthopedic, implant



**TABLE OF CONTENTS:****LIST OF TABLES****LIST OF FIGURES**

<b>General Introduction</b>	<b>12</b>
<b>1. Bones</b>	<b>15</b>
1.1. Introduction.....	15
1.2. Structure of Bone.....	16
1.3. Gross Anatomy of Bone .....	16
1.4. Classification of Bones .....	17
1.4.1. Shape.....	17
1.4.2. Composition and Structure.....	19
1.5. Fractures: Bone Repair .....	21
1.5.1. Types of Fractures .....	21
1.6. Bone Repair .....	22
1.7. Bone as a Mechanical Component .....	23
<b>2. Orthopedic implants</b>	<b>29</b>
2.1. Introduction.....	29
2.2. Types of orthopedic implants .....	29
2.2.1. Permanent orthopedic implants .....	29
2.2.2. Temporary orthopedic implants.....	30
<b>3. Biodegradable alloys for orthopedic implants</b>	<b>36</b>
3.1. Introduction.....	36
3.2. Magnesium Zinc alloys as biodegradable implants .	37
3.3. Designation system:.....	37
3.3.1. Magnesium.....	38
3.3.2. Zinc .....	40
3.3.3. Degradation of Mg-Zn alloys inside the human body.....	43
<b>4. Corrosion of Magnesium alloys</b>	<b>45</b>
4.1. Introduction:.....	45
4.2. The Body Environment .....	46
4.3. Corrosion Behavior .....	46
4.3.1. Electrochemical aspects.....	46

4.4. Degradation mechanisms .....	48
4.4.1. General Corrosion .....	48
4.4.2. Localized Corrosion.....	49
4.5. Different Mg-Zn alloys .....	49
4.6. In-Vitro Corrosion of Magnesium Implants in Various Simulated Physiological Environments.....	50
4.6.1. Influence of Inorganic Ions Present in the In-Vitro Electrolytes.....	51
4.6.2. Influence of Organic Components Present in the In-Vitro Electrolytes:.....	52
4.7. Protective Coatings to Improve the Corrosion Resistance of Magnesium Implants .....	52
4.7.1. Chemical coating.....	52
4.7.2. Physical coating.....	53
<b>5. Methods:</b>	<b>57</b>
<b>5.1. Diffusion-based Model.....</b>	<b>57</b>
<b>5.2. Finite element simulation.....</b>	<b>57</b>
5.2.1. Model simplification .....	57
5.2.2. Modeling.....	58
5.2.3. Meshing .....	59
5.2.4. Implementation.....	59
<b>6. Results:</b>	<b>62</b>
<b>6.1. Model calibration .....</b>	<b>62</b>
<b>6.2. Implant degradation.....</b>	<b>62</b>
6.2.1. Mass loss.....	65
6.2.2. Magnesium ions diffused in the body .....	67
6.2.3. Hydrogen evolution .....	68
6.2.4. Evolution of Hydroxide ions .....	70
6.2.5. Effective Young Modulus.....	71
<b>6.3. Possible solutions the encountered problems .....</b>	<b>72</b>
6.3.1. Alloying elements.....	72
6.3.2. Surface treatment and coating.....	72
<b>General Conclusion</b>	<b>74</b>
<b>References</b>	<b>76</b>

**LIST OF TABLES:**

TABLE 1.1 BONE CLASSIFICATION, THEIR FEATURES, FUNCTIONS AND EXAMPLES .....	19
TABLE 1.2 DIFFERENT TYPES OF FRACTURES AND THE DESCRIPTION OF EACH ONE .....	22
TABLE 1.3: PROPERTIES OF NATURAL BONE .....	26
TABLE 3.1 MAGNESIUM PROPERTIES .....	39
TABLE 3.2 PROPERTIES OF DIFFERENT IMPLANTS MATERIALS .....	39
TABLE 3.3 ZINC PROPERTIES .....	41
TABLE 6.1: MAGNESIUM CONCENTRATION AND YOUNG MODULUS OF ALLOYS. ....	62
TABLE 6.2: EMPIRICAL PARAMETERS OF POWER FUNCTION FOR SIMULATED ALLOYS .....	66
TABLE 6.3: EMPIRICAL PARAMETERS OF POWER FUNCTION FOR SIMULATED ALLOYS .....	67

## LIST OF FIGURES:

FIGURE 1.1: A TYPICAL LONG BONE SHOWS THE GROSS ANATOMICAL CHARACTERISTICS OF BONE .....	16
FIGURE 1.2: CLASSIFICATION OF BONES BASED ON SHAPE .....	17
FIGURE 1.3 TRABECULAR BONE AND COMPACT BONE.....	20
FIGURE 1.4: A COMPARISON BETWEEN A HEALTHY BONE AND DIFFERENT TYPES OF FRACTURES: (A) CLOSED FRACTURE, (B) OPEN FRACTURE, (C) TRANSVERSE FRACTURE, (D) SPIRAL FRACTURE, (E) COMMUNUTED FRACTURE, (F) IMPACTED FRACTURE, (G) GREENSTICK FRACTURE, AND (H) OBLIQUE FRACTURE.....	21
FIGURE 1.5 BONE HEALING PROCESS.....	22
FIGURE 1.6: TYPICAL STRESS-STRAIN CURVE FOR BONE, WITH ELASTIC AND PLASTIC REGIONS LABELED AS WELL AS YIELD AND FAILURE POINTS.....	26
FIGURE 1.7: MATERIAL EXPANDS IN A PERPENDICULAR DIRECTION WHEN LOADED IN COMPRESSION. THE PARAMETER THAT QUANTIFIES THIS PHENOMENON IS POISSON'S RATIO. ....	26
FIGURE 2.1: TOTAL HIP REPLACEMENT. ....	30
FIGURE 2.2: (A) PLATES, (B) SCREWS, (C) PINS, (D) WIRES, AND (E) INTRAMEDULLARY NAILS USED IN FRACTURE FIXATION .....	31
FIGURE 2.3: A SCHEMATIC DIAGRAM FOR THE DESIGN, ADDITIVE MANUFACTURING (AM), POST-TREATMENTS OF BONE SCAFFOLDS, AND SEVERAL TYPICAL AM-DERIVED SCAFFOLDS. ....	33
FIGURE 2.4: INTAMEDULLARY NAIL FIXED ON FEMUR BONE.....	34
FIGURE 3.1: THE SCHEMATIC DEPICTION OF IMPLANT DEGRADATION COINCIDES WITH AN INCREASE IN BONE LOADING CAPACITY. ....	37
FIGURE 3.2: CRYSTALLIZED MAGNESIUM .....	38
FIGURE 3.3: ZINC FRAGMENT SUBLIMED AND 1CM <sup>3</sup> CUBE.....	41
FIGURE 3.4: ASSESSED PHASE DIAGRAM OF THE MG-ZN SYSTEM .....	43
FIGURE 4.1: SCHEMATIC REPRESENTATION OF DIFFERENT TYPES OF CORROSION IN MAGNESIUM AND MAGNESIUM ALLOYS .....	48
FIGURE 5.1 STEPS OF MODEL SIMPLIFICATION.....	58
FIGURE 5.2 IMPLEMENTED MODEL GEOMETRY. ....	58
FIGURE 5.3: MESHING OF THE SIMULATION DOMAIN .....	59
FIGURE 5.4 SUB TREE OF THE TRANSPORT OF DILUTED SPECIES MODULE .....	59
FIGURE 5.5 SUB TREE OF THE DEFORMED GEOMETRY MODULE .....	60
FIGURE 5.6 REPRESENTATION OF THE THREE TASKS DONE IN EACH STEP	60
FIGURE 6.1 CONTOUR PLOTS OF THE IMPLANT DEGRADATION AND CORROSION ENVIRONMENT CONCENTRATION AT 0, 120, 240 AND 360 DAYS AFTER IMMERSION OF PURE MG.....	63

FIGURE 6.2 CONTOUR PLOTS OF THE IMPLANT DEGRADATION AND CORROSION ENVIRONMENT CONCENTRATION AT 0, 120, 240 AND 360 DAYS AFTER IMMERSION OF Mg-2Zn ALLOY. ....	64
FIGURE 6.3 CONTOUR PLOTS OF THE IMPLANT DEGRADATION AND CORROSION ENVIRONMENT CONCENTRATION AT 0, 120, 240 AND 360 DAYS AFTER IMMERSION OF Mg-4Zn ALLOY. ....	64
FIGURE 6.4 CONTOUR PLOTS OF THE IMPLANT DEGRADATION AND CORROSION ENVIRONMENT CONCENTRATION AT 0, 120, 240 AND 360 DAYS AFTER IMMERSION OF Mg-6Zn ALLOY. ....	65
FIGURE 6.5 CONTOUR PLOTS OF THE IMPLANT DEGRADATION AND CORROSION ENVIRONMENT CONCENTRATION AT 0, 120, 240 AND 360 DAYS AFTER IMMERSION OF Mg-8Zn ALLOY. ....	65
FIGURE 6.6: EVOLUTION MASS LOSS FOR SIMULATED ALLOYS.....	66
FIGURE 6.7: EVOLUTION MASS OF DISSOLVED MAGNESIUM FOR SIMULATED ALLOYS.....	67
FIGURE 6.8: EVOLUTION MASS OF DISSOLVED MAGNESIUM PER DAY FOR SIMULATED ALLOYS .....	68
FIGURE 6.9: EVOLUTION OF HYDROGEN GAS VOLUME FOR SIMULATED ALLOYS.....	69
FIGURE 6.10: EVOLUTION HYDROXIDE IONS QUANTITY FOR SIMULATED ALLOYS .....	70
FIGURE 6.11: EVOLUTION EFFECTIVE YOUNG'S MODULUS FOR SIMULATED ALLOYS.....	71

## General Introduction:

A decade ago, the biodegradable implants of bone fixation gained a lot of interest and had become a very important subject of study for biomaterials researchers. Between all the materials known, magnesium was one of the best choices for these implants thanks to the outstanding combination of its properties. The magnesium is very accepted by the human body, it can be degraded naturally over the time and its Young's modulus is close from that of the bone, furthermore it is very helpful when it comes to the bone healing. However, an optimal combination between mechanical and degradation properties must take place, thus, the use of specific addition elements in order to improve these properties, for instance: Zinc.

The different chapters of this manuscript are divided into two main parts .The first parts which contains four chapters is the bibliographical study of 'bones', 'orthopedic implants', 'Biodegradable alloys for implants' and 'corrosion of Mg alloys'. The second part is the experimental part where it was mainly about modelling and simulation of Mg-Zn implant.

The first chapter is about bones, it gives information about the structure, classification, composition and mechanical properties of bones.

The second chapter talks about the orthopedic implants, it reveals the different types of these implants as intramedullary nails, plates and screws and scaffolds.

The third chapter is biodegradable alloys for implants, this chapter talks mainly about Mg-Zn alloys, it also gives information about magnesium and zinc and their properties.

The fourth chapter is about the corrosion of Mg alloys, it shows the electrochemical behavior of these alloys in the human body and some simulated physiological environments.

The last chapter is the modelling and simulation of Mg alloys with the method of finite elements (FEM) for an intramedullary nail under conditions similar human body.

THEORETICAL  
PART

# CHAPTER 1

## Bones



## 1. Bones:

### 1.1. Introduction:

As the largest dynamic biological tissue in the body, bones are composed of inorganic minerals and metabolically active cells surrounded by a large volume of extracellular matrix, and they form a rigid framework that has an irreplaceable role in maintaining life activities, including supporting the body and protecting visceral organs.

Bones show a unique construction composed of an organic matrix, a mineral substance and cavities. In combination these three constituents respond to the environmental mechanical stresses. The bones mass-to-strength ratio is optimized by natural modeling and remodeling processes. Bones have different structures, depending on their location. The internal structure of a bone, for example, is very heterogeneous. The microstructure often evolves with sex, age, activities, etc...[1]. on average, bones are composed of 35% of organic matrix (mostly collagen fibrils (90%)) and 65% of mineral substances. .... [2]

The human skeleton is one of the most important systems in the body. Among its multiple functions, providing structural and mechanical support for the body is the most essential. Bone tissue adopts an optimal structural arrangement that enables it to meet the mechanical demands of the local environment. [3]

## 1.2. Structure of Bone

Bone structure is crucial to maintaining its role within the body. Bone tissue structure at various metric scales is surprisingly complex and Hierarchical. Human bones at the macroscopic level adopt different sizes and shapes that match their local environment and functional needs. Bone tissue (osseous tissue) is significantly different from other body tissues. Bone is rugged and depends on that characteristic hardness in many of its functions.

## 1.3. Gross Anatomy of Bone

The long bone structure enables best visualization of all parts of a bone. There are two parts to a long bone: the diaphysis and the epiphysis. The diaphysis is the tubular tube, flowing between the bone's proximal and distal ends. In the diaphysis the hollow region is called the medullary cavity, which is filled with yellow marrow. The diaphysis walls are made of compact, dense and strong bone (Figure 1.1).

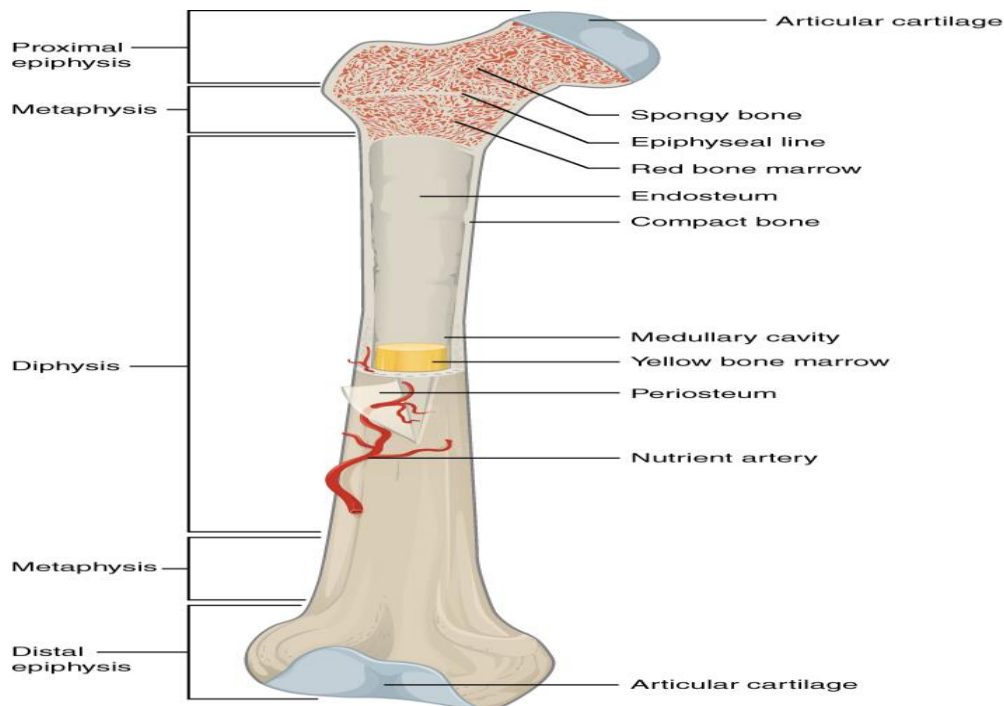


**Figure 1.1: A typical long bone shows the gross anatomical characteristics of bone**

At either end of the bone the larger portion is called the epiphysis which is filled with spongy tissue. The gaps in the spongy bone are filled with red marrow.

## 1.4. Classification of Bones

Depending on their sizes, the 206 bones that make up the adult skeleton are divided into five categories while there are two other categories classified according to their composition and structure. The shapes and functions are related in such a way that each categorical bone shape has a distinct function.

### 1.4.1. Shape

According to the shape we do have five categories which are mentioned in Figure 1.2.

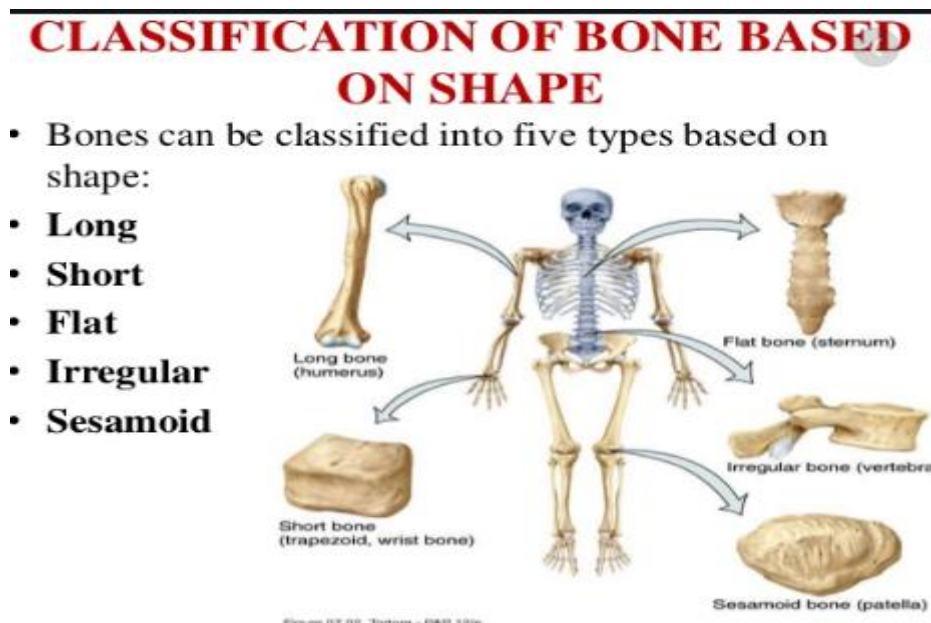


Figure 1.2: Classification of bones based on shape

#### 1.4.1.1. Long Bones:

A long bone is one in shape which is cylindrical, being longer than it is wide. Nevertheless, bear in mind that the word defines a bone's shape, not its scale. The arms (humerus, ulna, and radius) and legs (femur, tibia, and fibula) as well as the fingers (metacarpals, phalanges) and the toes (metatarsals, phalanges) contain long bones. Long bones serve as levers; as muscles contract, they shift.

#### 1.4.1.2. Small Bones:

A short bone is one in shape like a cube, being about equal in length, width and thickness. The only short bones within the human skeleton are in the wrist carpals and the ankle tarsal. Short bones, as well as some limited motion, provide stability and support.

#### 1.4.1.3. Flat Bones

The word "flat bone" is a bit of a misnomer since, while a flat bone is normally smooth, it is sometimes curved too. The cranial (skull) bones, scapulae (shoulder blades), sternum (breastbone), and ribs are examples. Flat bones act as attachment points for muscles and also shield internal organs.

#### 1.4.1.4. Irregular Bones

An irregular bone is one that has no easily defined shape and thus suits no other classification. These bones tend to have more complex forms, such as the vertebrae supporting the spinal cord and protecting it against compressive forces. Many facial bones are classified as abnormal bones, particularly those containing sinuses.

#### 1.4.1.5. Sesamoid Bones

A sesamoid bone is a thin, round bone, shaped like a sesame seed, as the name implies. These bones develop in tendons (the tissue sheaths that link bones with muscles) where a lot of pressure is produced in a joint. Through helping them withstand compressive forces, the sesamoid bones secure tendons. The number and location of sesamoid bones vary from person to person, but are usually located in tendons associated with the feet, hands, and knees. The patellae (singular = patella) are the only sesamoid bones common to anyone.

**Table 1.1 Bone classification, their features, functions and**

Bone classification	Features	Functions	Examples
Long	Cylinder-like shape, longer than it is wide	Leverage	Femur, tibia, fibula, metatarsals, humerus, ulna, radius, metacarpals, phalanges
Short	Cube-like shape, approximately equal in length, width, and thickness	Provide stability, support, while allowing for some motion	Carpals, tarsals
Flat	Thin and curved	Points of attachment for muscles; protectors of internal organs	Sternum, ribs, scapulae, cranial bones
Irregular	Complex shape	Protect internal organs	Vertebrae, facial bones
Sesamoid	Small and round; embedded in tendons	Protect tendons from compressive forces	Patellae

**examples**

#### 1.4.2. Composition and Structure:

According to the composition and structure of the bone we find two categories:

##### 1.4.2.1. Cortical (compact) bone:

The cortical bone, consisting of 80 per cent of the total bone mass, is a densely packed bone layer that constitutes the outer shell of all bones. Cortical bone surrounds and covers the cavity inside. Its rigid and dense structure determines the form of the bone and gives the bending and torsion resistance that can result from external force. Cortical bone thickness can vary considerably across different sites, and is often affected by external factors such as exercise and disease. The cortical bone thickness in the human sacrum, a piece of bone situated at the bottom of the spine and connected to the pelvis, can range from 0.5 to 2.25 mm [4]. Nevertheless, cortical thickness can be 34.9 per cent higher in the dominant arms of tennis players than in the contralateral arm [5]. Typically thinner cortices are reported in an aging population[6].

## 1.4.2.2. Trabecular (spongy) bone

Trabecular bone, is highly porous. It is composed of a highly complex network of individual trabeculae which either assume a shell-like structure, known as trabecular plates, or a beam-like structure. Many tissues such as bone marrow, blood vessels, and nerves penetrate trabecular bone within the cortical bone layer. Although it consists of just 20 % of the overall bone mass, trabecular bone accounts for the bulk of the bone surface area, for one total surface area around  $7\text{m}^2$ . In addition, trabecular bone location varies greatly between different bones, even within different locations of the same bone. In long bones, the trabecular bone, known as the epiphysis and metaphysis, is concentrated at the enlarged bone ends. The ratio between cortical bone and trabecular bone content in the femoral head, the proximal end of the femur inserted into the hip, is approximately 50:50. Nevertheless, the diaphysis (long-bone midshaft) is dominated by cortical bone. For example, the human radius diaphysis, one of two long bones in the forearm, has as little as 5 percent of a trabecular portion. [6].

Figure 1.3 illustrates the trabecular bone as well as the compact bone in a long bone.

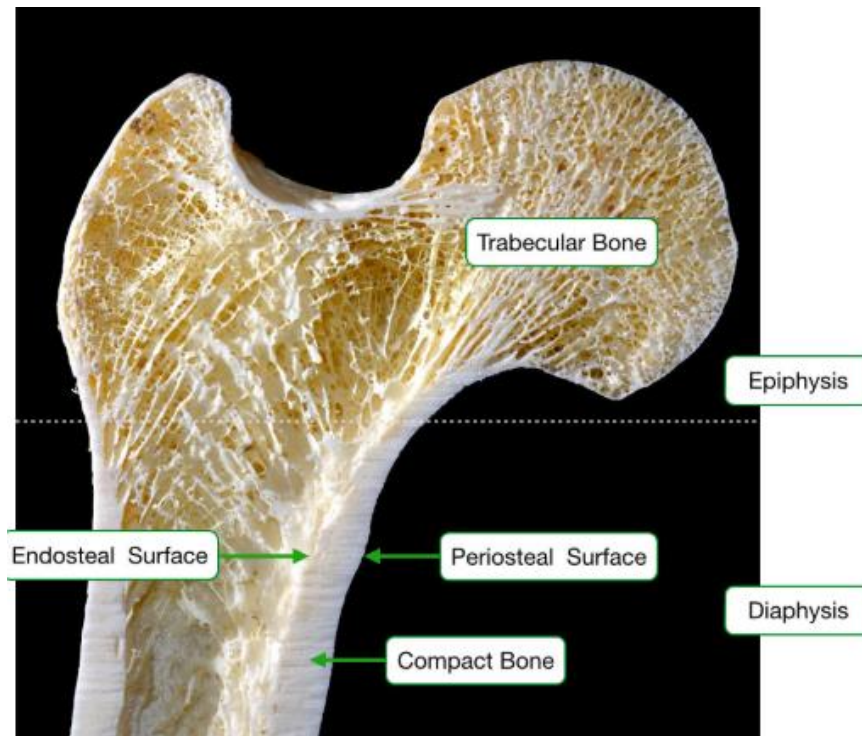


Figure 1.3 Trabecular bone and Compact bone

### 1.5. Fractures: Bone Repair:

A broken bone is a fracture. It will heal whether a doctor resets it in its anatomical position, or not. If the bone is not properly repaired, the healing process holds the bone in its deformed location.

If a fractured bone is repaired without surgery and replaced in its normal place, the operation is considered a closed reduction. Open reduction requires surgery to expose and reset the bone to the fracture. Although some fractures may be minor, others are quite severe and cause serious complications.

#### 1.5.1. Types of Fractures:

Fractures are classified according to their complexity, location and other characteristics that outline common types of fractures. Some fractures can be defined using more than one term since they may have characteristics of more than one type ( e.g. an open transverse fracture) (Figure 1.4)

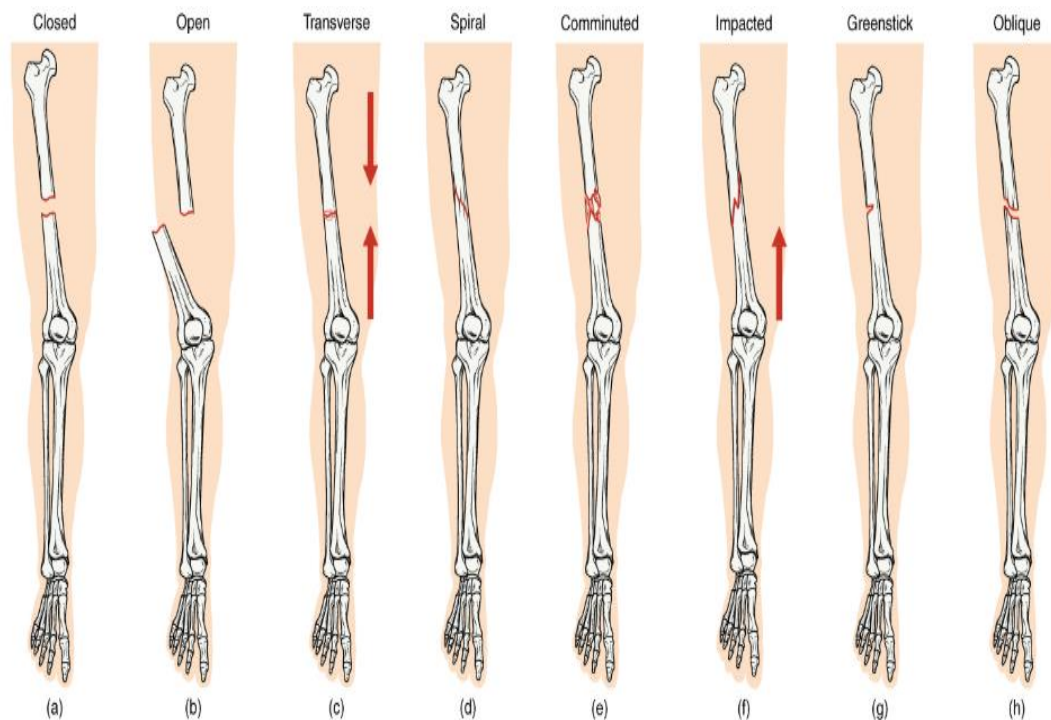


Figure 1.4: A comparison between a healthy bone and different types of fractures: (a) closed fracture, (b) open fracture, (c) transverse fracture, (d) spiral fracture, (e) comminuted fracture, (f) impacted fracture, (g) greenstick fracture, and (h) oblique fracture.

**Table 1.2** different types of fractures and the description of each one

Type of fracture	Description
Transverse	Occurs straight across the long axis of the bone
Oblique	Occurs at an angle that is not 90 degrees
Spiral	Bone segments are pulled apart as a result of a twisting motion
Comminuted	Several breaks result in many small pieces between two large segments
Impacted	One fragment is driven into the other, usually as a result of compression
Greenstick	A partial fracture in which only one side of the bone is broken
Close (simple)	A fracture in which the skin remains intact
Open (compound)	A fracture in which at least one end of the broken bone tears through the skin; carries a high risk of infection

### 1.6. Bone Repair:

If a bone fractures, there is a complicated restoration mechanism at the fracture Location. A brief description of the key steps in this process will be given in the Next part. Figure 1.5 outlines the process of repairing a broken bone. The healing process can be differentiated by four different steps [7]:

- Hematoma formation.
- The development of fibro cartilaginous calluses.
- Bone callus.
- Bone Remodeling.

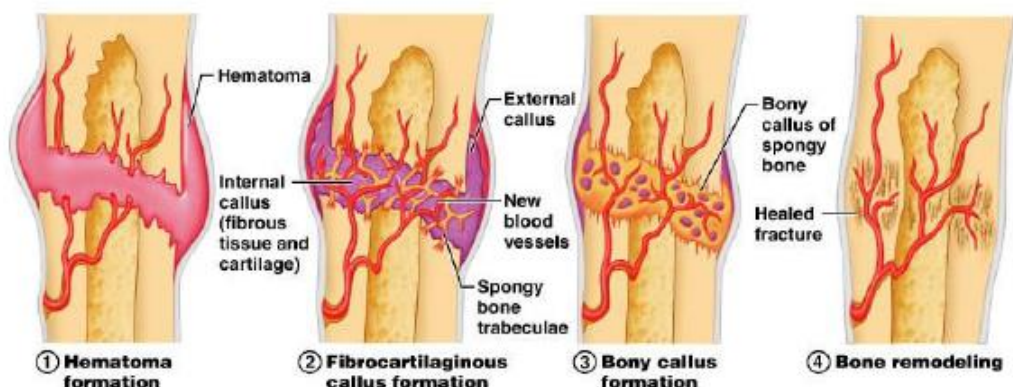


**Figure 1.5** Bone healing process [8]



The first step, (1), occurs immediately after the fracture. This refers to an equivalent inflammatory reaction to the reaction to anybody injury. There is an increase in blood flow, which enables different cells to move around the bone edge. It is worth noting that an infection has the highest probability of occurring during this stage, particularly in the case of an open fracture. Antibiotics are frequently used to prevent such scenarios. The standard medical treatment is drugs (antibiotic) but currently under consideration antibacterial coatings are innovative ideas. Silver coatings for example are designed to be used on medical implants as bactericidal. It was shown that silver coatings resist bacterial adhesion or colonization. [9] The inflammatory activity has a peak within 24 H and is complete after 7 days [10].

Cell proliferation and differentiation followed by the production of new fibrous connective tissue matrix (especially collagen fiber) occurs during the second step, (2). This new tissue is known as soft callus. During the first 4 to 6 weeks of the healing process this tissue can't support load application.

During the third step, (3), the soft callus becomes stiffer and is transformed into the hard callus.

The final stage, (4), can last several years during which the bone is slowly repaired after having experienced mechanical stresses to increase the ratio of mass- to- strength.

In mobility, bones can need to be re-aligned and restricted depending on the severity of the injury. Mechanical stability is obtained by means of devices (plates, rods, pins and screws).

### 1.7. Bone as a Mechanical Component

One of the bone's most significant role is to sustain body weight and protect soft tissue around it. Bones need to be able to tolerate deformation and dissipate load onto other areas of the body in the face of external forces and impacts to avoid serious injury. They serve as a muscle attachment site through tendons and enable the transfer of muscle-generated force to body movement. Even when the body stands still or seated, the bones and the skeleton provide the body with a support structure. The primary feature of the bones is thus mechanically guided and relies on the bone's mechanical integrity.[10]

The material usually undergoes physical deformation ( $\Delta L$ ) when a force (F) is applied on a material. Within, particles that make up the body undergo an internal physical quantity called stress(s), usually

quantified by the normalized (divided) force exerted by the cross-sectional area ( $A$ ) of the body perpendicular to the direction of force [11]:

$$\sigma = F/A$$

Likewise, the original dimension of the body ( $L$ ) will normalize the external deformation, yielding a geometry-independent volume of deformation named strain  $\varepsilon$ :

$$\varepsilon = \Delta L/L$$

Higher orders of magnitude of force, deformation, stress, and strain typically exert greater mechanical demands on the object. A variety of quantitative mechanical metrics were devised to characterize the mechanical quality of the bone based on these values. For example, bone stiffness ( $S$ ) is determined by dividing force by displacement across a piece of bone along the same axis on which the force is applied [12]:

$$S = F/\Delta L$$

Hence, it defines the ability of the bone to resist deformation under external force. Bone with higher stiffness will bend less with the same force compared with one with lower stiffness. Additionally, elastic modulus ( $E$ ), also known as Young's modulus, is determined by the stress and strain ratio and supports the bone's material-level potential to endure force deformation, regardless of external geometry:

$$E = \sigma/\varepsilon$$

The bone strength, another widely used bone consistency metric, can be described as the peak force that a bone can sustain until it begins failing. In comparison, bone resilience measures bone's ability to withstand energy and resist fracturing. A variation of these factors is usually quantified at the same time in order to better understand the mechanical nature of bone.

Since various parts of the body undergo different degrees of mechanical stress, bone at different locations has different mechanical properties that are appropriate for their local function. Vertebral bodies, the materials that make up the skeleton, are often undergoing compressive loads as the top and bottom surfaces are moving each other along [13]. Even the vertebral bodies differ from one another at different locations.

Bone tissue properties are well described. The stress-strain behavior of the bone undergoes several stages under a constant load. In the initial stage, bone functions as a linear elastic material, where stress is linearly

correlated with strain, resulting in a constant elastic module calculated as the slope of the stress-strain curve. In this area, it takes the same amount of additional stress to achieve a given strain increase. As strain continues to rise, stress will increase until a critical point known as yield stress, where the material property begins to deviate from the linear elastic region to the non-linear region, also known as the plastic region. (Figure 1.6)

The stress-strain curve slope will begin to decrease, leading to a lower elastic modulus. It is because the input stress caused the bone content to break physical and chemical bonds, resulting in micro fractures that weaken the bone. To achieve a given increase in strain, less additional stress is required. Eventually, as the load continues to rise, microfracture in the bone accumulates to the point of complete failure of the bone and no longer sustaining the load, a point known as failure (Figure1.6)

The normal mechanical activity of bone under load usually exists in the linear region under physiological conditions, because the rates of in vivo strain are generally low. Therefore, many bone tests apply only small stress or strain to measure the elastic module in the linear area, and do not surpass the yield point. The bone specimen is still intact in this case, and can still be processed for further studies. Previous studies have found that cortical bone elastic modulus is about 18 GPa while trabecular bone is about 15 GPa [14]. In comparison, the stainless steel and silicone rubber elastic modulus are 200 and 0.05 GPa, respectively. [15]

The Poisson ratio ( $\nu$ ), which describes the phenomenon of a material expanding in a perpendicular direction when loaded in compression, is another important mechanical parameter. Vice-versa, when pulled in tension the material contracts perpendicularly. The negative ratio of transverse strain to axial strain can be defined as this. Most materials have a Poisson ratio between 0 and 0.5, given that 0.5 is an incompressible material. Bone usually has a ratio of 0.3 to Poisson [16](Figure1.7 ).

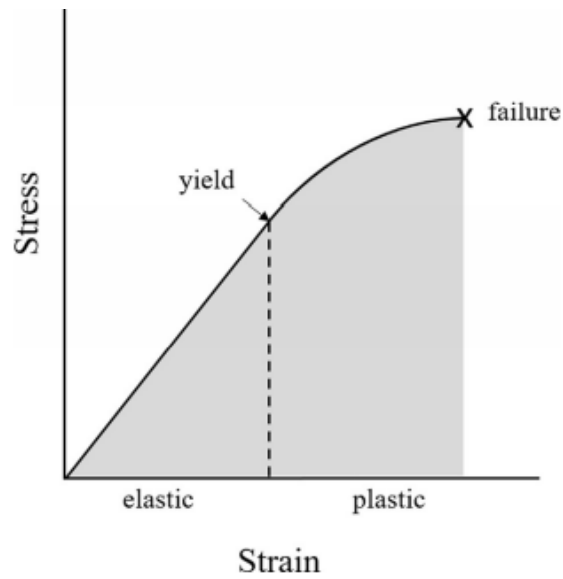


Figure 1.6: Typical stress-strain curve for bone, with elastic and plastic regions labeled as well as yield and failure points.

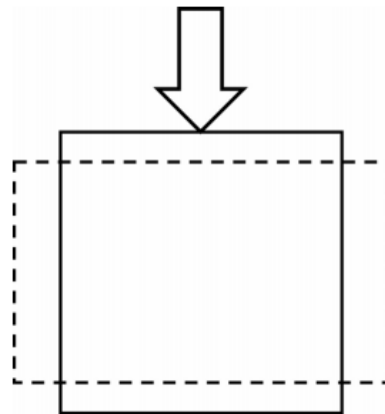


Figure 1.7: Material expands in a perpendicular direction when loaded in compression. The parameter that quantifies this phenomenon is Poisson's ratio.

Table 1.3: Properties of natural bone [15]

Properties	Natural Bone
Density ( $\text{g}/\text{cm}^3$ )	1.7-2.0
Elastic Modulus(GPa)	3-20
Compressive Yield Strength (MPa)	130-180
Tensile Strength (MPa)	80-150
Elongation at failure (%)	1-7

These parameters can quantify the material properties of bones, and the properties can be summarized for isotropic materials by their young modulus and the ratio of Poison.

# CHAPTER 2

## Orthopedic implants

## **2. Orthopedic implants:**

### **2.1. Introduction:**

People with injuries and joint conditions such as osteoarthritis, rheumatoid arthritis and post-traumatic arthritis may need surgery that requires implants such as complete replacements to the hip and knee. Orthopedic implants include instruments and parts for temporary fracture repair, such as plates, screw pins, wires and nails. Because orthopedic implants have to operate in vivo under various working conditions, a thorough understanding of the basic needs of orthopedic materials and biological response is essential to the design and optimization of implants in the human body. In orthopedic implants metal alloys, ceramics, and polymers are widely used. These materials have numerous physical, chemical, and biological properties that are suitable to particular applications. Metallic alloys, for example, are commonly used in load-bearing joint prostheses and devices for repairing bone fracture due to the strong mechanical properties, while ceramic materials with superior wear resistance and bioactivity are sometimes used as articulating parts or bioactive coatings on implants. Polymers typically act as a barrier between joints to minimize friction and attachment devices. The demand for improved orthopedic materials in this area has spurred considerable progress leading to the design and manufacture of orthopedic implants with higher performance and new properties.

### **2.2. Types of orthopedic implants:**

#### **2.2.1. Permanent orthopedic implants:**

Various forms of total joints are commonly used as substitutes, including the hip, knee, arm, back, elbow, wrist and finger joints[17]. Throughout the patients' life cycle these permanent orthopedic implants are required to work in the human body, and metals, ceramics, and polymers are widely used. Hip and knee joint prostheses in particular have undergone rapid growth and medical acceptance in the last few years. But the delicate articulation and complicated transfer of load make it very difficult to build such prostheses. A standard complete hip substitute consists of a stem, a femoral head, a liner and an acetabular cup (Figure 2.1).



**Figure 2.1: Total hip replacement.**

### 2.2.2. Temporary orthopedic implants:

#### 2.2.2.1. Plates and screws:

The other type of orthopedic implants are temporary ones which are required during the healing process to repair broken or damaged bones. Temporary orthopedic implants, including plates, screws, pins, wires, and intramedullary nails[17] (Figure 2.2) can operate for a relatively short period of time, only long enough to allow bones to heal. Plates of various shapes and sizes containing holes for screws and pins are used to bind plates to bones, enough so bone fragments can be compressed together throughout the load-bearing bones healing operation. Together with other instruments, screws are widely used particularly for fixing the associated instruments to bones and also as stand-alone components for fixing broken fragments. Pins may be used as adjunctive fixing devices in complex bone fracture along with other devices to withstand a strong load, or used alone just to repair fractures under relatively weak force. As simple but flexible implants, wires are widely used to hold together bone fragments as well as to re-attach the larger trochanter in long oblique / spiral long bone fractures or hip replacements. An intramedullary nail is a surgical rod that is inserted into the medullary canal of a long bone to serve as an immobilization device to keep the two ends of the long broken bone in place. In general, other implants such as



pins or screws are placed into predrilled holes in the rods to hold the nails in place within a piece of bone.

One major problem of the healing of bone fixed with rigid plates is bone weakening due mainly to the stress-shielding effect that can lead to refracture after removal of the plate. The stress-shielding effect of permanent prosthetic implants is also a major concern. The osteogenic (bone generating) and osteoclastic (bone removal) processes in the human bones are considered to be natural activities. As defined in Wolff's law[18], if a greater load is applied to the bone over a period of time, the osteogenic process is more productive and provides better load support. In comparison, a decreased bone load causes bone mass loss. Biodegradable materials such as metallic alloys[19, pp. 1–34] and polymers[20, pp. 2335–2346] with a structure similar to that of the bone have attracted considerable attention as potential bone fixing devices. Free from the shielding effect, bone cure is encouraged, and natural implant degradation allows the human body to progressively reduce implant strength and eventually absorb it. There is no need for a follow-up surgery to remove the repairing devices after recovery, thus lessening patient pain and reducing health-care costs. However, due to issues such as rapid degradation this solution is still in the infancy stage, and further study is required to make the materials clinically appropriate.

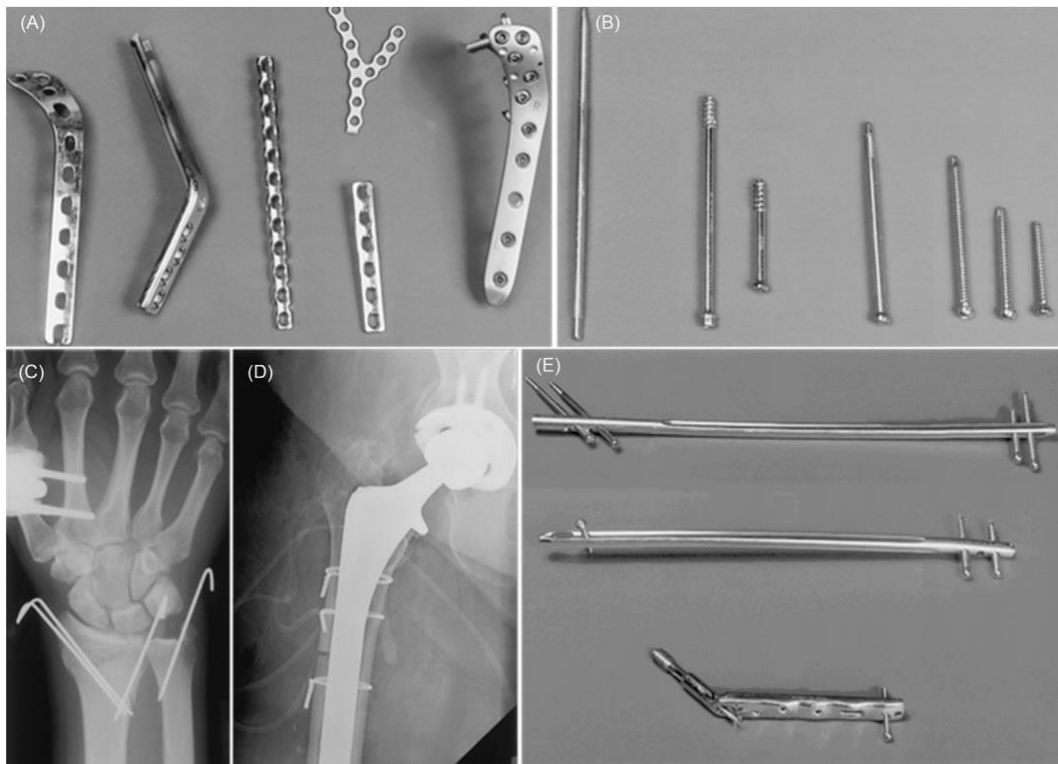


**Figure 2.2: (A) Plates, (B) screws, (C) pins, (D) wires, and (E) intramedullary nails used in fracture fixation[21, pp. 1569–1590]**  
 2.2.2.2. Biodegradable Scaffolds

Biodegradable scaffolds are generally considered as indispensable elements for engineering living tissues as they are used as temporary templates with specific mechanical and biological properties similar to native extracellular matrix (ECM). They allow modulating cell adhesion, invasion, proliferation and differentiation, prior to the regeneration of biologically functional tissue or natural ECM. The most effective way to produce these scaffolds is the Additive Manufacturing (AM).

Additive manufacturing (AM) can produce a porous scaffold with individual external shape and porous internal structure [22]. Before AM +with desired architecture using computer-aided design (CAD) software. The 3D scaffold model is sliced into a series of two-dimensional (2D) slices before converting to typical Stereolithography (STL) files, which contain detailed 2D slice information. Based on these STL files, an AM machine performs the necessary tool path along the 2D directions for direct building of 2D layers. Each layer is just built on top of the other to construct a 3D part. Due to the fabrication process of adding one layer on the previous one, this manufacturing technique is described as AM. Currently, researchers around the world are committed to apply AM techniques to produce porous implants for bone repair. For instance, Poukens[[23] successfully applied AM to fabricate porous mandible implant, which was subsequently implanted in a patient. Brazilian Jardim et al.[24] used an AM processed customized porous scaffold to repair a large cranial defect. Australian Peter implanted the AM-derived porous titanium implants into a 71-year-old patient who faced an amputation of the heel bone. All these successes positively render the AM techniques a promising future for bone tissue repair.

A typical application of porous scaffolds fabricated by AM includes the scaffolds design, AM, and post-treatments, as schematically illustrated in Figure 2.3.

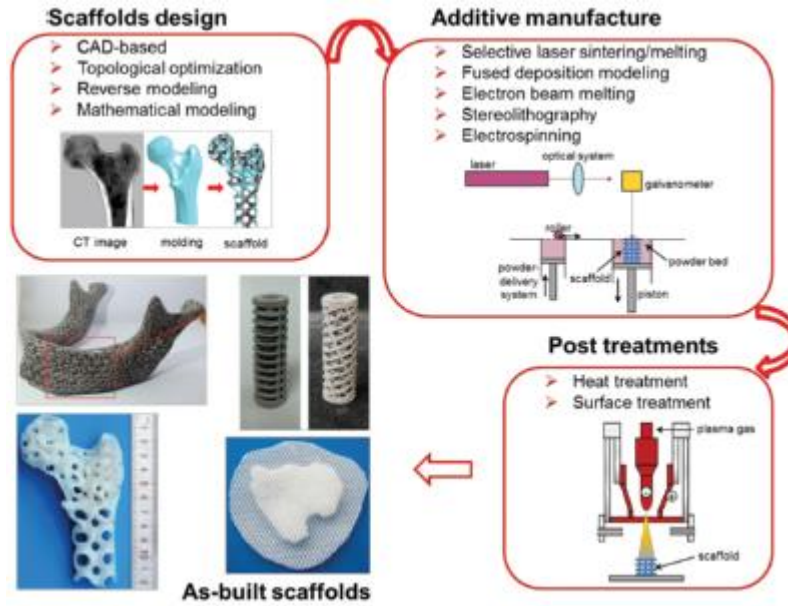


**Figure 2.3: A schematic diagram for the design, additive manufacturing (AM), post-treatments of bone scaffolds, and several typical AM-derived scaffolds. [25]**

Therefore, this work reviews the overall process for AM of bone scaffolds. Several typical structure design methods are first examined, especially the mathematical modeling method, which can achieve with both bionic design and topological optimization of scaffolds. Following on, the most relevant AM techniques using for scaffolds fabrication, with their advantages and disadvantages, are highlighted. The common post-treatments related to AM-derived scaffolds are also discussed. Finally, the future trends for AM scaffolds for bone repair are addressed.

### 2.2.2.3. Intramedullary nails:

Intramedullary devices (IM nails) are used as internal struts to stabilize long bone fractures. Intramedullary nails are also used for fixation of femoral neck or inter-trochanteric bone fractures; however, this application requires the addition of screws. Many designs are available, going from solid to cylindrical, with shapes such as cloverleaf, diamond and C (slotted cylinders). Compared with plates, IM nails are better positioned to resist multidirectional bending, since they are located in the center of the bone. However, their torsional resistance is less than that of plates. Therefore, when designing or selecting an intramedullary nail, a high polar moment of inertia is desirable to improve torsional rigidity and strength. The torsional rigidity of an IM nail is proportional to the elastic modulus and to the moment of inertia. For nails with a circular cross-section, torsional stiffness is proportional

to the fourth power of the nail's radius. The wall thickness of the nail also affects the stiffness.

In addition to the need to resist bending and torsion, it is vital for an IM nail to have a large contact area with the internal cortex of the bone to permit torsional loads to be transmitted and resisted by shear stress.

These intramedullary nails can be made of different materials, for the none-biogradable implants stainless steel and titanium are the best choices for this use. However, for the biodegradable intramedullary nails, the ones made of magnesium are very interesting.

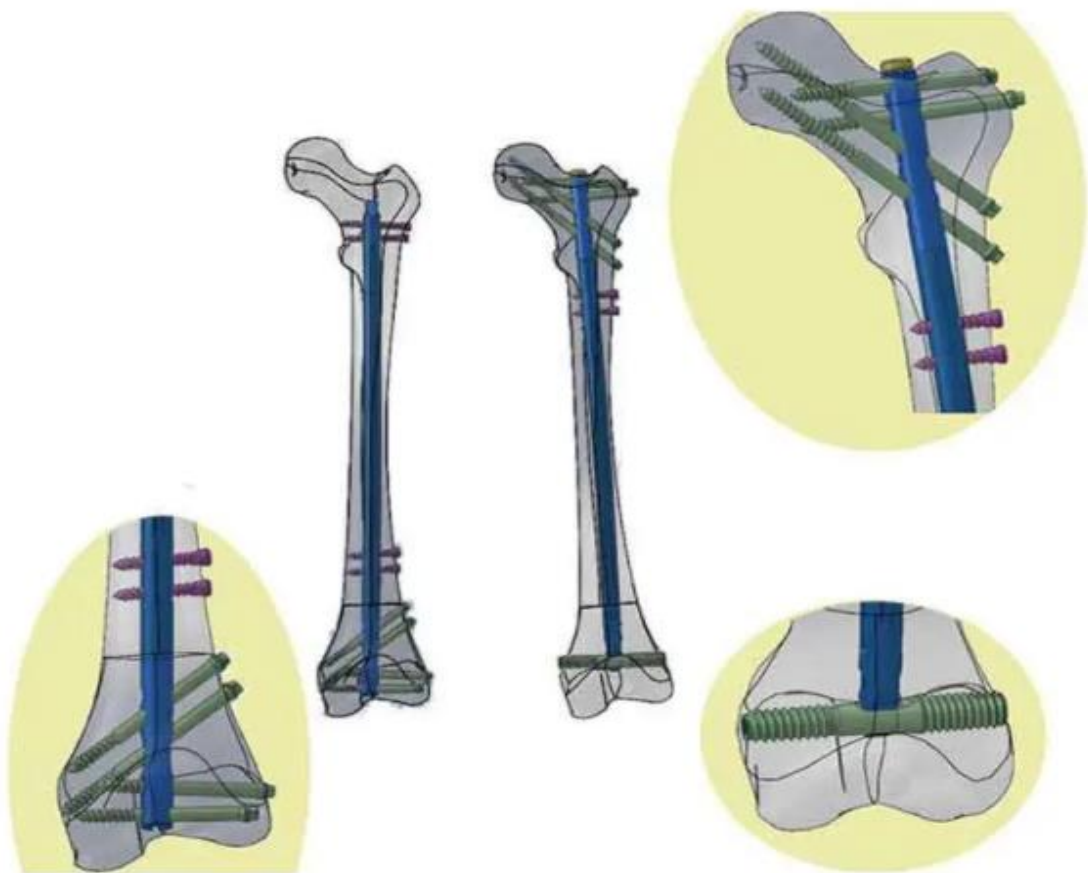


Figure 2.4: Intamedullary nail fixed on femur bone

# CHAPTER 3

## Biodegradable alloys for orthopedic implants

### 3. Biodegradable alloys for orthopedic implants

#### 3.1. Introduction:

Throughout most of the history of materials, most of the metals were used as permanent implant materials for treating broken bones and wound closure and they were chosen on the basis of experimental trials in the surgical field. The key idea for the temporary application of metal implants was first historically documented by the Romans who used metal clips to heal skin wounds[26]. There are various materials used at the beginning of osteosynthesis, such as gold, silver, platinum, copper, lead and iron[26]. Such metals were refused for surgical use for a number of reasons. Gold and platinum are advantageous from the point of view of corrosion resistance, but they're quite expensive and at the same time have bad mechanical properties, while lead is rejected due to its toxicity. Silver and iron are generally considered to be suitable biomaterials[26]. However, mechanically pure silver is not sufficient for osteosynthesis. Other critical discussions on the biocompatibility of iron have also taken place since metallosis was observed following the implantation of iron implants. Metallosis is seen as infiltration of periprosthetic soft tissue and bone by metal debris due to wear and tear of joint replacements. Metallosis is often associated with severe osteolysis. The identification of metallosis is therefore an indication for revision surgery[27]. These clinical observations have led to the paradigm that metal implants must be truly resistant to corrosion.

Artificial bone grafts are developed to reduce the risk to the patient and the financial cost. The objective is to develop an implant that is as similar as possible to bone characteristics[28, pp. 131–140] [29, pp. 26–36]. The advantage is that artificial bone grafts can be made as large as much as necessary. In addition, patient and location-specific implants can be designed. The structural, surface and material properties can lead to achieving osteoconductivity, osteoinductivity and osteogenity. Degradable bone substitute materials are developed in this way. Degradation of the implants enables the bone to replace it during the healing period. Therefore, the implants remain in the body only as long as necessary and do not need to be removed. As a result, financial and physical burdens can be reduced. In addition, the implants lose the stiffness associated with the healing period. This can be controlled by alloy elements and coatings [30, pp. 1729–1799] [31]) Bone growth is induced in this way. In Figure 3.1 the mechanical interaction between the implant and the bone during the healing period is represented schematically. Optimally, the stiffness of the implant-bone

compound remains stable, while the load is gradually shifted from the implant to the bone.

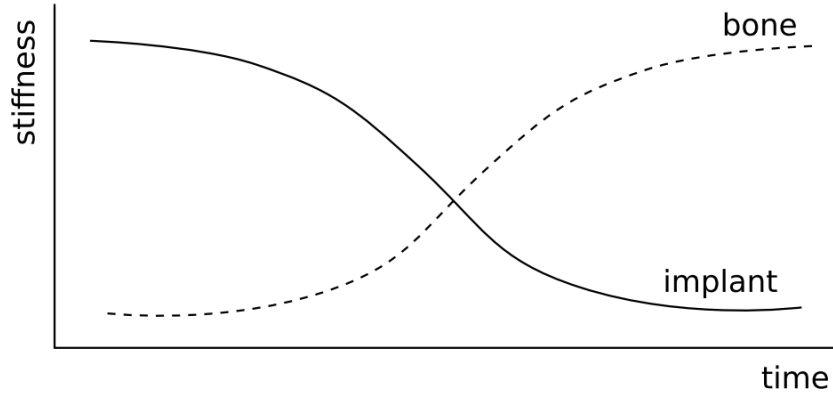


**Figure 3.1: The schematic depiction of implant degradation coincides with an increase in bone loading capacity.**

### 3.2. Magnesium Zinc alloys as biodegradable implants:

To date, polymeric materials are being used as degradable implants, but they might cause inflammation and wound healing disorder [32, pp. 3413–3431] [33]. Magnesium alloys have proved to be a promising alternative due to their high biocompatibility, excellent mechanical properties and controllable degradation behavior. Magnesium alloys possess two main advantages. In the first place, magnesium occurs naturally in the human body. Second, magnesium is among the lightest metals with a density of  $1.74 \text{ g.cm}^{-3}$  and a modulus of elasticity of 44 GPa which are very close to bone properties ( $1.8\text{--}2.1 \text{ g.cm}^{-3}$  and 3–20 GPa respectively)[34] [29]. As a result, the stress on the bone is not completely covered by the implant and the effects of "stress shielding" that can lead to bone resorption are reduced[35, pp. 124–134]. These two factors make magnesium alloys extremely desirable for clinical applications[31].

### 3.3. Designation system:

There's no designation system has universal acceptance. Names of alloys have evolved from trade names of the pioneering companies to chemical and numerical systems.

Most of the modern researches uses the designation (Mg-XZn) where X is the weight fraction of Zinc in the alloy, so we will use the same designation.

### 3.3.1. Magnesium:

Magnesium was discovered by Sir Humphrey in 1808, but it took a hundred years for a real market for magnesium to grow. The uses of magnesium as a building material have been very limited, mainly used as an alloy element in aluminum alloys. Or other marginal applications, such as steel deoxydant, chemicals and pyrotechnics, but rarely in structural uses[36].

Magnesium is considered an alkaline-earth metal. It is found in group 2 and period 3 of the periodic table. Therefore it has an electronic structure similar to Be, Ca, Sr, Ba and Rd.

Magnesium is the sixth most abundant element in the earth's crust, accounting for 2.7% of the earth's crust [37]. After lithium, it is the lightest of metals since it has a density of around 1.74 g / cm<sup>3</sup>, which represents a quarter of the density of steel and two thirds of that of aluminum[38] [39].



**Figure 3.2: Crystallized magnesium**



3.3.1.1. Magnesium Properties

**Table 3.1 Magnesium Properties[36] [40]**

Atomic Number	<b>12</b>
Atomic Weight ( <i>g</i> )	24.3050
Crystal Structure	hexagonal close-packed: $a = 3.2092 \text{ \AA}$ $c = 5.2105 \text{ \AA}$
Density ( <i>g.cm<sup>-3</sup></i> )	1.738 at 20 °C 1.65 at 650 °C
Melting Point (°C)	650
Boiling Point (°C)	1090
Upon Melting there is a volume increase of 4.2%	
its mechanical properties are quite weak, which is why it is used in the form of alloys.	

3.3.1.2. Medical applications:

Magnesium alloys were introduced as orthopedic biomaterials in the first half of the last century[41]. However, due to their poor corrosion resistance, a large amount of hydrogen accumulates around the implant during the corrosion process in vivo, limiting the use of magnesium-based materials as biomaterials. Despite this, magnesium still has many attractive characteristics that make magnesium-based materials potential candidates as implants in some applications in the medical sector [40].

Magnesium has a much lower density than other implant materials (Table 3.2). It also has greater fracture toughness compared to hydroxyapatite. In addition, as shown in Table 3.2 , its elasticity and compressive strength values are much more comparable to those of natural bone than materials commonly used as implants[42].

**Table 3.2 Properties of different implants materials[42]**

Material	Density ( <i>g.cm<sup>-3</sup></i> )	Tenacity ( <i>MPa.m<sup>1/2</sup></i> )	Elastic modulos ( <i>GPa</i> )	Compressive strength( <i>MPa</i> )
Human Bones	1.8 – 2.1	3 – 6	3 – 20	130 – 180
Ti Alloys	4.4 – 4.5	55 – 115	110 – 117	758 – 1117
Co-Cr Alloys	8.3 – 9.2	-	230	450 – 1000
Stainless Steel	7.9 – 8.1	50 – 200	189 – 205	170 – 310
Magnesium	1.74 – 2.0	15 – 40	41 – 45	65 – 100
Hydroxyapatite	3.1	0.7	73 – 117	600

Magnesium has good biocompatibility and is biodegradable the human body, thus eliminating the need for another operation to remove the implant. This makes magnesium alloys promising materials as a biodegradable implant [42] [43]. In recent years, much research has been done in order to overcome the corrosion problems which limit the use of magnesium-based materials in the field of orthopedics, research mainly focused on the use of different alloying elements and the development of protective coatings on these alloys[42].

### 3.3.1.3. Magnesium in the human body:

Magnesium (Mg) is the fourth most abundant mineral in the human body and is also essential for good health. In the human body, about 50% of Mg is found in the bones, 49% is found in the cells of body tissues and organs, and only 1% exists in the blood, a level which remains relatively constant and which is very important for the function of the blood. It is considered to play hundreds of roles in the nervous system, muscle function, bone strengthening as well as some important implications in the body, with, among other things, regulating the relaxation and contraction of muscles, production of protein and even the production and transport of energy throughout the body. According to previous research, those who drank water low in Mg were more likely to contract cardiovascular disease, revealing the important role of Mg in preventing cardiovascular disease. In addition, Mg content is considered a parameter related to asthma, kidney disease, diabetes, hypertension and a number of chronic diseases. Magnesium is often included in foods. The recommended daily intake of dietary magnesium is 400-420 mg per day for men and 310-320 mg per day for women with higher demands based on certain criteria such as age. Although the dosage of magnesium in serum is relatively stable, there is always a chance that humans have a deficiency or excess of magnesium. Magnesium levels in the blood are a condition associated with morbidity and mortality, especially in patients with co-morbidities[44].

### 3.3.2. Zinc:

Zinc is considered a post-transition metal. It is found in group 12 and period 4 of the periodic table. It is part of the "zinc group", so it has an electronic structure similar to Cd, Hg and Cn.

For chemists, the zinc group is clearly distinguished from alkaline earths, with metals insoluble in water, having fairly low melting and boiling points, low ionic radii, and having a tendency to form complexes.

Zinc is in some respects similar to magnesium in that its current oxidation state is +2, resulting in a cation comparable in size to  $Mg^{2+}$ . And it is the 24th most abundant element in the earth crust.



Figure 3.3: Zinc fragment sublimed and  $1cm^3$  cube

### 3.3.2.1. Zinc Properties

Table 3.3 Zinc Properties[45]

Atomic Number	<b>30</b>
Atomic Weight ( <i>g</i> )	65.37
Crystal Structure	hexagonal close-packed: $a = 2.6649A^\circ$ $c = 4.9468 A^\circ$
Density ( $g.cm^{-3}$ )	7.14 at 20 °C 6.83 at 650 °C
Melting Point (C°)	419.4
Boiling Point (C°)	907
Zinc has a hexagonal crystal structure which cannot be changed.	
Zinc is a relatively dense metal at 7.14 g / ml, and has a low melting point.	
Its mechanical properties are poor	

### 3.3.2.2. Zinc in the human body:

Zinc, with a density of approximately  $7.14 g.cm^{-3}$ , is one of the essential and most abundant metallic elements in the human body, and is important for over 300 different enzymes. Biologically speaking, it is essential for cell metabolism, protein support, DNA synthesis, and the senses of taste and smell. For adults, the recommended dietary allowance of Zn is approximately 10 to 15 mg per day, larger amounts are often considered relatively non-toxic; almost 100 mg per day can be tolerated for some time[44].

### 3.3.2.3. Magnesium Zinc alloys:

Zinc, as an alloying element in magnesium alloys can improve ductility and deformability. Additionally, the introduction of Zn into these alloys can increase tensile strength and hardness through a solid solution hardening mechanism, as well as aging hardening. The Zn element can also decrease certain impurities such as iron and nickel, which improves corrosion resistance properties.

The binary phase diagram is shown in (Figure 3.4). According to the diagram, it can be seen that the maximum solid solubility of Zn in Mg is about 6.2% by mass at the eutectic temperature of 341 ° C. In recent decades, three groups of Zn-Mg alloys for different applications have been reported.

The first group includes alloys containing less than 6% Zn, which is below the solubility limit. Many binary Mg-Zn alloys with different proportions are distinguished, such as Mg-0.5Zn, Mg-1Zn, Mg-1.5Zn, Mg-2Zn, Mg-3Zn, Mg-4Zn, Mg-5Zn, Mg-6Zn. The microstructure of these alloys consists mainly of solid  $\alpha$ -Mg solution, which improves formability and machinability at elevated temperatures. Thus, alloys with low Zn content can be hot machined into their final form.

The second group of Zn-Mg-based alloys has a chemical composition that is close to the eutectic point in the Zn-Mg system, exhibiting a high amorphous formation capacity. Alloys in this group can easily form in an amorphous structure, when there is rapid cooling.

The third group represents zinc-based alloys, where the Mg concentration is limited[44].

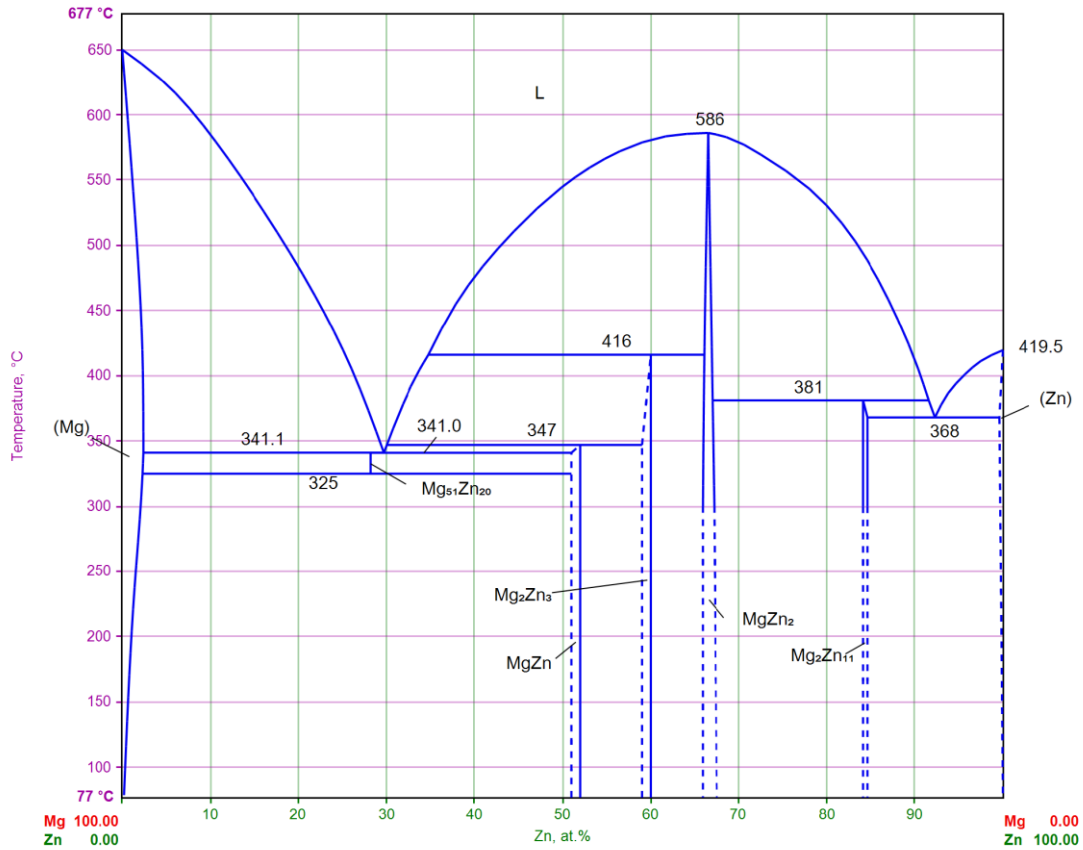


Figure 3.4: Assessed Phase Diagram of the Mg-Zn System[44]

### 3.3.3. Degradation of Mg-Zn alloys inside the human body:

The corrosion behavior of Mg-Zn alloys strongly depends on the Zn content and the distribution of the Mg-Zn phase. The standard potential of Zn is  $-0.762$  V, which is significantly nobler than Mg ( $-2.37$  V). In addition, Zn is characterized by a relatively high potential for hydrogenation, and the addition of Zn to Mg alloys can increase this potential. Thus, the addition of zinc can improve the corrosion resistance of Mg alloys. On the other hand, the distribution of Mg-Zn precipitates causes micro galvanic corrosion and therefore an increase in the corrosion rate of these alloys. Also, the corrosion products of Mg-Zn binary alloys are too weak at the surface to protect against corrosion [44].

# CHAPTER 4

## Corrosion of Magnesium alloys

## 4. Corrosion of Magnesium alloys:

### 4.1. Introduction:

Magnesium (Mg) or its alloys are commonly tested as possible orthopedic implants, especially because bio-degradable alloys for fracture fixation are similar to those of bone due to their mechanical properties. Due to its rapid degradation and associated degradation products, currently available Mg or its alloys face challenges in passing regulatory biosafety tests prior to clinical trials. Mg degradation is followed by Mg ion release, pH increase, and osmolality in surrounding environments. Pursuant to the ISO 10993 Part 13 standard, the pH value shall be appropriate for the site of intended use being maintained within an appropriate range. Approaches to overcome these obstacles include choosing suitable alloying elements, proper surface treatment techniques and monitoring the rate of degradation of Mg or its alloys as orthopedic implants formed. Mg or its alloy-based bone implants have not yet been widely used as therapeutic implants in clinical applications. One of the alloying elements which is commonly used is Zinc (Zn).

Magnesium (Mg) is a reactive metal and corrosion protection is an issue of importance.[46], the high intrinsic dissolution tendency of magnesium, which is only weakly inhibited by corrosion product films, and [47] the presence of second phases acting as local cathodes and thus causing local micro-galvanic acceleration of corrosion .Recently however, corrosion is a positive attribute for Mg alloys for use as biodegradable implants.[48]

## 4.2. The Body Environment

The human body's water content varies from 40 to 60 per cent of its total mass. The overall body water can biologically be subdivided into two main fluid compartments, namely the extracellular and the intracellular fluids. Extracellular fluids (ECFs) consist of plasma present in the blood vessels, interstitial fluid surrounding the cells, lymph and transcellular fluids (e.g., cerebrospinal fluid, and joint fluids). Intracellular fluid (ICF) is the water inside the cells. Both the volume and the distribution of body fluids and electrolytes, a process known as homeostasis, are kept regular and stable. Electrolytes play a key role in the functionality of the body. They participate in metabolism among various functions, determine the cell membrane potential and body fluid osmolarity, and so on. Major cations include ions such as hydrogen, sodium, potassium, calcium and magnesium. Major anions include ions such as hydroxide, bicarbonate, chloride, phosphate and sulphate. The most important components for in vivo implant corrosion are possibly the dissolved salts. Chloride ions (and other halides) accelerate corrosion of virtually any metal and interfere with other corrosion safety methods.[49]

Temperature and pH are two major factors that influence materials' corrosion behaviour. Body fluids have a temperature of 37 C, under normal conditions. This can be used as a steady temperature in spite of corrosion during an implant's lifetime.[50]

## 4.3. Corrosion Behavior

Magnesium is commonly known to have low efficiency in corrosion. This activity is one of the reasons why magnesium is a successful candidate for use in biodegradable implants. Since corrosion mechanisms depend heavily on the environment, then corrosion behavior in a body fluid must be investigated for biomedical applications. Specific mechanisms involving bacteria or living cells are also expected. Certainly these aspects of in vivo corrosion must be regarded.[51]

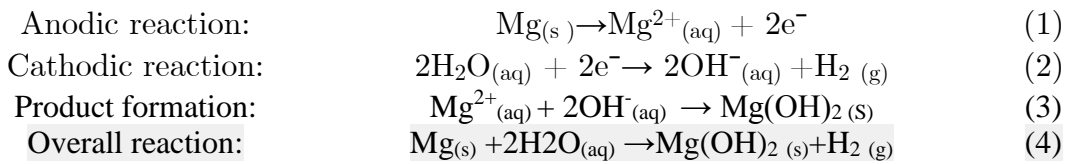
### 4.3.1. Electrochemical aspects

A metal's corrosion is due to an exchange of electron between the material and an external chemical compound. A double layer capacitor may appear after a dynamic equilibrium of the corrosion reaction has been established. It is formed by two charged layers, one in the substance due to metal dissolution, and the other at the surface by ion attraction to the surface in the solution. Instead, there is a possible gap between those two layers. [52]



## CHAPTER 4: Corrosion of Magnesium alloys

The probable difference determined in standard conditions (Standard conditions correspond to pure element sample in molar solution of the metal ions under 1bar pressure.) between the pure metal sample and a stable reference electrode is called the standard electrode potential. It reflects a metal's propensity to be oxidized: the equilibrium on the oxide production side is displaced for low value of this potential. Compared to other metals such as silver (0.8 V), aluminum (-1.7 V) or iron (0.56 V), the standard potential (versus hydrogen) for magnesium (-2.37 V) is weak. This means that magnesium is highly reactive and has a strong oxidation propensity. Because of that high reactivity, the following reactions occur when magnesium is in contact with an aqueous solution:

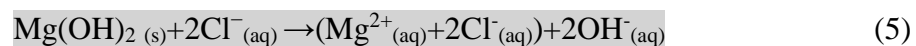


The kinetics properties of these reactions can be substantially modified, depending on environmental parameters such as temperature, pH, and species activity in solution or ion adsorption on the surface. [53]

Magnesium corrosion is accompanied by hydrogen gas release and the formation of hydroxide compounds may produce a film on the surface.

When this film is formed under atmospheric conditions; the surface of a magnesium sample turns to grey. Under standard atmosphere and in a high alkaline solution (pH > 10.5) this film is stable.[54]

Because of various phenomena this film is usually unstable under other conditions. First, the misfit between the structure of the magnesium crystal and its hydroxide induces stresses in the film layer that can lead to cracks in the film [55]. Furthermore, hydrogen development will result in the decoherence of portions of the film for the immersed samples [55]. Eventually, the film is dissolved in aqueous solutions containing chloride, so that the surface is safe for corrosion [55]. The presence of chloride ions quickly converts the hydroxide layer into highly soluble magnesium chloride [56]



The disappearance of the hydroxide layer due to chloride ions hastens the corrosion of magnesium alloys. Additionally, hydrogen gas (H<sub>2</sub>) evolution during magnesium corrosion can create subcutaneous gas bubbles [57] and gas bubbles adjacent to the implants, which can cause

the separation of tissues and/or tissue layers [58]. In-vitro studies report the critical tolerance level of hydrogen to be  $<0.01$  mL/day, and this has been widely used to screen magnesium alloys for temporary implant applications [58]. However, it should be noted that each alloy must be investigated in-vivo in relation to the intended function. In this context, it may be interesting to note that a few in-vivo studies [59] have reported the evolved hydrogen-forming gas pockets only in the first week post-surgery, which gradually disappear over a period of 2–3 weeks post-surgery. Thus, it may be reasonable to assume that hydrogen evolution may not significantly interfere with the healing process as long as the corrosion rates of the magnesium implants are appropriately controlled in the first couple of weeks, such that the hydrogen evolution rate remains lower than 0.01 mL/day.

#### 4.4. Degradation mechanisms:

Mechanisms of corrosion can be classified into two parts: general corrosion (as well called uniform corrosion) and localized corrosion. The magnesium alloys were reported in both categories. Figure 4.1 displays a schematic representation of various potential mechanisms for corrosion in magnesium alloys.

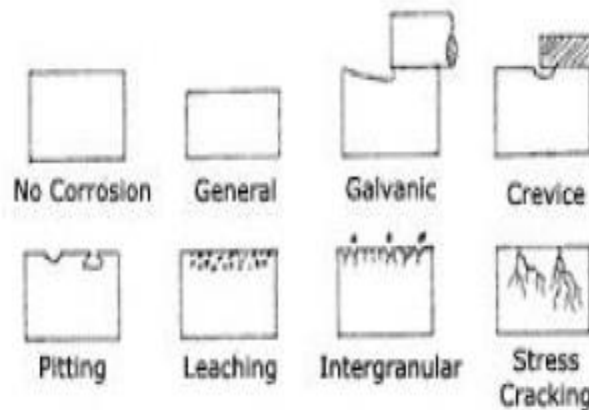


**Figure 4.1: Schematic representation of different types of corrosion in magnesium and magnesium alloys**

##### 4.4.1. General Corrosion:

As its name suggests, a general corrosion is a corrosion that occurs homogeneously over the entire surface of the sample. The kinetics of the corrosion reactions and/or the diffusion process [60] govern this kind of corrosion. On a naked metal, without any corrosion product, the corrosion rate is determined by the slowest chemical reaction if the adsorption of reactive elements on the surface is rapid. But if the

corrosion products are not dissolved and start forming clusters, and eventually a film, it will be more difficult to adsorb ions to the surface, then the rate of corrosion that slow. Depending on film resistance and porosity the film on the surface may be protective with performance [61].

#### 4.4.2. Localized Corrosion

Localized corrosion usually occurs because the material is heterogeneous. In the most common phenomenon of magnesium alloys with a high negative effect on corrosion resistance is the micro-galvanic effect due to alloying elements. Pure magnesium is generally alloyed to improve its mechanical properties by strengthening the solids, precipitation or particles. From a chemical viewpoint however, the microstructural heterogeneities arising from the added elements (clusters, precipitates, particles of the second phase) are typically more cathodic than magnesium. Thus a micro-galvanic cell may be formed between the matrix of magnesium and the precipitates [62]. The particles play the role of cathodic areas with magnesium dissolution occurring at the interface. This form of corrosion will eventually cause the particles to fall out [63]. The second phases present in the magnesium matrix could lead to a dramatic degradation due to this micro-galvanic effect.

Pitting is a particular localized corrosion mechanism that occurs in magnesium. As mentioned earlier, the film for the corrosion product may not be stable. When the film breaks at some point, the naked material is in direct contact with the solution, thereby allowing ion exchange [64]. The exposed area becomes anodic and the metal dissolves; the wide region covered with the film serves as a cathodic area [64]. Pitting can also occur as a result of the preferential corrosion of the second phase areas. In some alloys of Mg-Al, Mg-Zn used as implants where second phases such as AlMn, AlZn, Mg<sub>17</sub>Al<sub>12</sub> or Mg<sub>x</sub>Zn<sub>y</sub> act as a cathode, corrosion pitting can also be noticed. [65]

As micro-galvanic corrosion occurs at grain boundaries for precipitates or segregation of materials, this is called intergranular corrosion. Microstructural characterisation of the sample surface may allow a pitting mechanism or an intergranular corrosion to be identified.

To identify ways to improve the corrosion resistance of magnesium implants in the presence of a physiological environment, it is important to investigate their corrosion rates and mechanisms. Magnesium alloy in-vitro corrosion has been thoroughly investigated in a variety of simulated physiological solutions which are outlined in the following sections.

#### 4.5. Different Mg-Zn alloys

Zinc (Zn) is one of the most abundant essential nutrients in the human body and is safe for use in biomedical applications [66]. The rate of Mg corrosion can be reduced by increasing the mass fraction of Zn mixed with Mg, thus strengthening the mechanical properties of Mg through solid solution hardening. Cai et al. reported that a Zn content of up to 5 wt.% in Mg-Zn binary alloys exhibits grain boundary, solid solution, and secondary phase strengthening, resulting in improved resistance to corrosion and mechanical properties [67]. Mg-6Zn alloy has good biocompatibility *in vitro* based on hemolysis.

Due to having a combination of good mechanical properties and corrosion resistance, some commercial Mg alloy systems have been selected as biodegradable Mg alloys at an early stage. Commercial Mg alloys used in biological research include the AZ (Mg-Al-Zn) and ZK (Mg-Zn-Zr) series alloys.

AZ series alloys, particularly AZ31 (Mg-3Al-1Zn) and AZ91 (Mg-9Al-1Zn) alloys, have been extensively studied both *in vitro* and *in vivo* in recent years [68]. It has been reported that AZ31 and AZ91 alloys release hydrogen upon degradation in physiological environments, leading to a significant increase in both pH and Mg ion concentration [69]. In Hank's solution, the AZ31 alloy degrades more slowly than the AZ91 alloy, but there is no significant difference *in vivo* [70]. Short-term *in vivo* studies of AZ31 and AZ91 alloys have also revealed that a biocompatible Ca phosphate protective film layer covers their surfaces and increases the formation of new bone mass around the implants [71].

Recently, ZK series alloys, especially ZK40 (Mg-4Zn-0.5Zr) and ZK60 (Mg-6Zn-0.5Zr), have attracted the attention of researchers because of the good biocompatibility of the component elements [72]. A daily intake of 11 mg Zn and 50  $\mu$ g Zr is permissible, so Mg-Zn-Zr alloys are more attractive than Mg-Al-Zn and Mg-RE-Zr alloys in terms of element biocompatibility and biosafety and are candidate biodegradable metals for use in bone repair devices [73].

#### **4.6. In-Vitro Corrosion of Magnesium Implants in Various Simulated Physiological Environments:**

Magnesium alloy corrosion depends significantly on the ions present in the electrolyte. Corrosion of magnesium alloy has been investigated in a variety of *in-vitro* electrolytes which mimic the physiological fluid composition. Different corrosion rates and mechanisms have been

observed for a variety of magnesium implants according to the different ion concentrations in these electrolytes. [74]

The most commonly employed in-vitro electrolytes are Hank's solution, Ringer's solution, Dulbecco's Modified Eagle's Medium (DMEM), phosphate-buffered saline (PBS), original simulated body fluid, conventional simulated body fluid (c-SBF), ionized simulated body fluid (i-SBF), revised simulated body fluid (r-SBF), and modified simulated body fluid (m-SBF).[75]

Due to their near similarity in composition with blood plasma (i.e., inorganic ion concentration) numerous SBFs have been widely used by the in-vitro electrolytes.

Additionally, SBF on a variety of substrates can promote bone-like apatite formation [76]. Hank's balanced salt solution (HBSS) is one of the most prominent amongst other in-vitro electrolytes. HBSS has a high nutritional value [77] and is commonly used to support a variety of cell cultures in biomedical research [78]. A major difference between SBF and HBSS in the case of SBF is the presence of a buffering additive. In general, the buffering additives can form complexes with calcium ions ( $\text{Ca}^{2+}$ ) [79] that interfere with a metallic implant's corrosion process.

#### 4.6.1. Influence of Inorganic Ions Present in the In-Vitro Electrolytes:

The presence of inorganic ions present in the in-vitro electrolytes can have a major impact on magnesium implant corrosion rate. In general, the presence of chloride ions ( $\text{Cl}^-$ ) rapidly dissolves a hydroxide layer ( $\text{Mg}(\text{OH})_2$ ) that forms on the surface of a magnesium alloy. The high concentrations of ( $\text{Cl}^-$ ) in the blood plasma as well as in the in vitro electrolytes explain the rapid corrosion of magnesium implants. Sulphate ions ( $\text{SO}_4^{2-}$ ) are also known to accelerate magnesium implant corrosion. At the other hand, bicarbonate ions ( $\text{HCO}_3^-$ ) can form an insoluble carbonate in large amounts ( $> 27 \text{ mmol L}^{-1}$ ), which can passive the surface of the magnesium.

Low phosphate ion concentrations ( $\text{HPO}_4^{2-}$ ) can also decelerate corrosion of magnesium through the formation of insoluble and dense phosphates. Apart from these anions, inorganic cations can also cause magnesium corrosion in in-vitro electrolytes. The presence of calcium ions and phosphate ions could lead to the formation of calcium phosphate, which can significantly delay the corrosion kinetics when precipitated on the surface of the magnesium[80].

#### **4.6.2. Influence of Organic Components Present in the In-Vitro Electrolytes:**

While in most in-vitro experiments the electrolytes did not contain organic components, they are contained in appreciable amounts by the real blood plasma. Hence, understanding the effect of the most prominent organic components present in blood plasma on magnesium alloy corrosion resistance is significant. The most common organic components in blood plasma include proteins, glucose, fatty acids, and cholesterol. Proteins are well known to adsorb on the surface of a metal and may retard the corrosion of a metallic implant[81], as Yamamoto et al. also reported[82]. They related this to protein adsorption on the metallic implant surfaces, which serves as a barrier to corrosion, and greatly decreases magnesium implant corrosion.

#### **4.7. Protective Coatings to Improve the Corrosion Resistance of Magnesium Implants:**

Various techniques, including alloying [83], surface modification using energetic radiation and conversion coatings have been used to enhance magnesium alloys' corrosion resistance. Among these the most widely used strategy is the application of conversion coatings. Biocompatibility and strong barrier properties are the main requirements a coating must meet to use the coated magnesium alloys as implants. Various conversion coatings that were produced to improve the corrosion resistance of magnesium implants are summarized in the following section.

##### **4.7.1. Chemical coating:**

Chemical modifications are defined as new phases covering the surface of Mg alloys that are synthesized through chemical or electrochemical reactions. This method removes the native oxide layer that has fewer passive properties, such as an inability to efficiently protect against corrosion, but forms easily due to the high reactivity of Mg matrix. Chemical modifications generally include acid etching, alkaline heat treatment, fluoride treatment, anodic oxidation, and microarc oxidation (MAO) [84].

##### **4.7.1.1. Acid etching:**

A pretreatment method commonly used to remove the coarse scale produced during manufacturing and replace the native oxide layer with a more compact passivated layer [85]. Turhan et al. reported that acid etching with a 2.5%  $H_2SO_4$  solution greatly enhances the resistance of AZ91D alloys to degradation [85].

#### 4.7.1.2. Fluoride treatment:

Fluoride treatment of Mg alloys replaces the original oxide film with a thin and more homogeneous  $\text{MgF}_2$  layer with higher polarization resistance. The advantages of the  $\text{MgF}_2$  layer include a high density, low water solubility, and nontoxicity when fluorine ions are released into the host organism.

#### 4.7.1.3. Micro Arc oxidation (MAO):

MAO is a high-voltage plasma-assisted anodic oxidation process that is widely employed to modify the surface of biodegradable Mg alloys. MAO coatings are very hard and have good wear resistance, moderate corrosion resistance, and better thermal stability and dielectric properties.

#### 4.7.2. Physical coating:

##### 4.7.2.1. Polymer coatings

They are also promising Mg alloy modifications for use in orthopedic applications. Gray-Munro et al. explored the influence of polymer coating on the corrosion rate of AZ31 Mg alloy in SBF using PLA, which is a semi-crystalline biodegradable polymer, and found that the coating prevented corrosion, especially during the early stages of implantation [86].

##### 4.7.2.2. Laser surface processing

It uses a high-energy laser beam, has also been employed to regulate biodegradation of Mg alloys and has been found to cause secondary phase dissolution and create a fine grained structure. Coy et al. found significant dissolution of the second phase of  $\text{Mg}_{17}\text{Al}_{12}$  in AZ91D when using laser surface processing. Similar results were reported by Guo et al. and Khalfawi et al. for ZE41 alloys using laser processing. Appreciable improvements in resistance to corrosion have also been observed for the aforementioned modified alloys [87].

##### 4.7.2.3. Cold spray technology

A viable method for surface engineering of Mg alloys. The deposition of cold spray coatings involves ballistic impingement of particles, usually ranging in size from 1 to 100  $\mu\text{m}$ , accelerated by a high-velocity gas stream and sprayed towards the substrate surface. A low temperature process, cold spray is particularly suitable for the deposition of bioactive coatings on Mg alloys, making it possible to depress oxidation and phase

transformation of the substrate. Noorakma et al. recently studied the deposition of HA on an AZ51 alloy using a modified cold spray process and found that this modification helped retain the characteristics of HA. Immersion in SBF for up to 14 days revealed that HA-coated AZ51 alloy was bioactive and facilitated apatite formation [88].



EXPERIMENTAL  
PART

# CHAPTER 5

## Methods

## 5. Methods:

### 5.1. Diffusion-based Model:

The degradation of magnesium zinc alloys is shown to be uniform in experimental results, Thus this phenomena can be modeled using Fick's law, according to which the diffusion is governed by the equation:

$$\frac{\partial C}{\partial t} = -\nabla \cdot (D\nabla C)$$

where  $C$  is the concentration of diffused ions,  $t$  is the time,  $D$  the diffusivity and  $\nabla$  is the gradient, referring to the conventional single species model [89].

The concentration of ions in the solid magnesium depends on the modelled alloy, the value of  $C_{Mg}$  can be calculated through the equation:

$$C_{Mg} = \frac{\rho_{Mg}(1-w)}{M_{Mg}}$$

Where  $\rho_{Mg}$  is the density of pure magnesium,  $w$  is the mass fraction of alloying elements and  $M_{Mg}$  the molar mass of magnesium. And the value of  $C_{env}$  depends on the medium.

The diffusivity would vary depending on the medium, and due to the corrosion layer being a thin film it is negligible compared to the size of the corrosion medium, for simplification we will not take the corrosion layer into account in our stud. The diffusivity accounts for all the unknown effects in the phenomena so it will be determined by tests to best fit the experimental results.

### 5.2. Finite element simulation:

The model can be implanted in the finite element analysis software COMSOL Multiphysics using the predefined Transport of Diluted Species (tds) physics for a 2D structure problem, the challenge in numerically solving this problem is the movement of the solid liquid interfaces which produce a moving boundary problem, so we need to use the Deformed Geometry (dg) physics as well.

#### 5.2.1. Model simplification:

The model would be created to simulate a femur intramedullary nail, its section is almost identical throughout its length, so we can simplify it as a cylinder of  $10mm$  diameter and  $410mm$  length.

Since we considered the corrosion to be uniform across the medium we can reduce the model to a 2D horizontal section of the intramedullary nail, the model consist of a circle of  $10\text{mm}$  diameter.

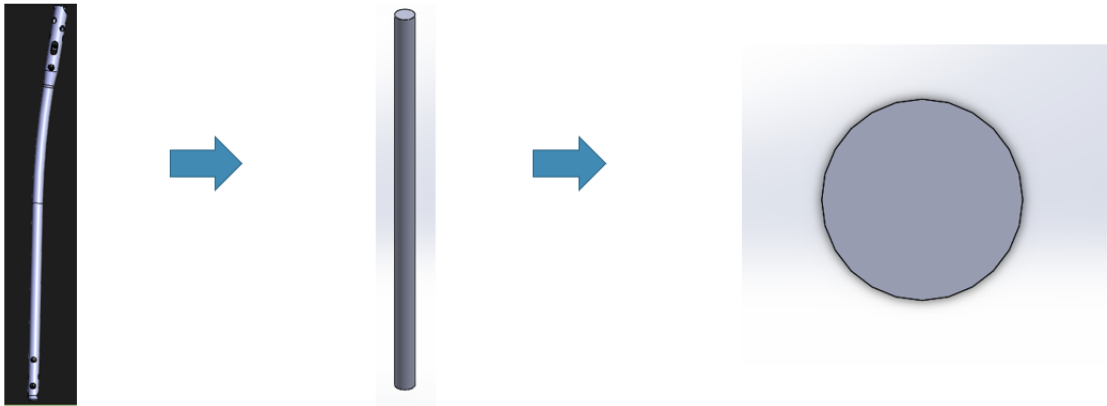


Figure 5.1 steps of model simplification

### 5.2.2. Modeling:

the problem was modeled the as two domains as shown in figure 5.2, the circle represent the implant and the square is the biological body, the dimensions of the square were chosen by trial and error, we started with  $20\text{mm}$ ; and went up until the concentration gradient became clearer at  $30\text{mm}$  wide.

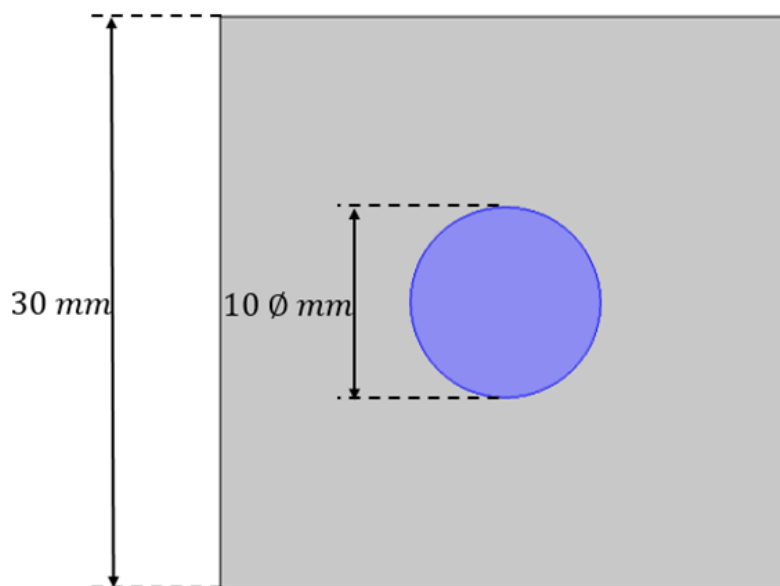


Figure 5.2 Implemented model geometry.

### 5.2.3. Meshing:

A fine free triangular mesh of 1.6mm size was used to discretize the domain, the mesh was made to get finer the closer it gets to the corrosion interface as shown in figure 5.3, because the concentration gradient steps are large there and if we didn't make the mesh finer the study might not converge.

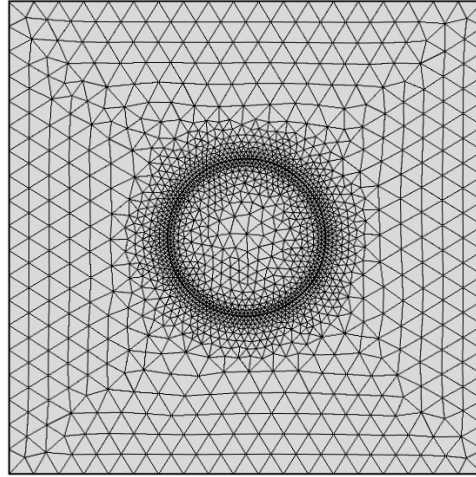


Figure 5.3: Meshing of the simulation domain

### 5.2.4. Implementation:

For the implementation the Transport of diluted species predefined Comsol physics model was used, the model depends on Fick's law of diffusion, we needed to implement the initial values of the concentrations for the two domains and the transport properties which are the diffusion coefficients of the two domains, and we specified the no flux boundary as the sides of the square so there won't be any exchange with the exterior environment.

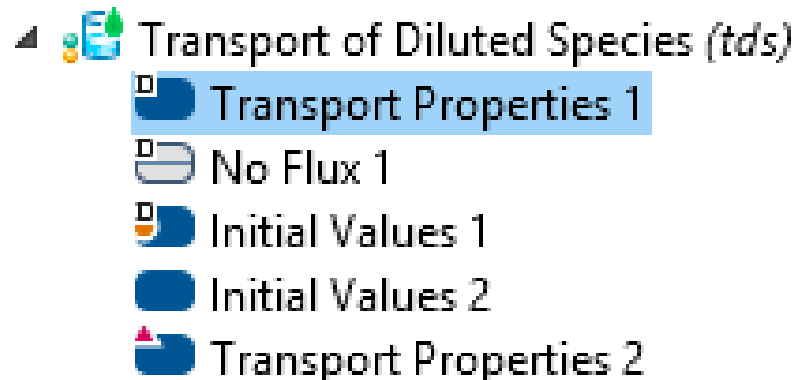


Figure 5.4 Sub tree of the Transport of Diluted Species Module

In order to solve the moving boundary problem we used Deformed Geometry mathematics module (dg), mathematical methods were used to calculate the velocity of the deformed corrosion interface, and then it was implemented in the module.

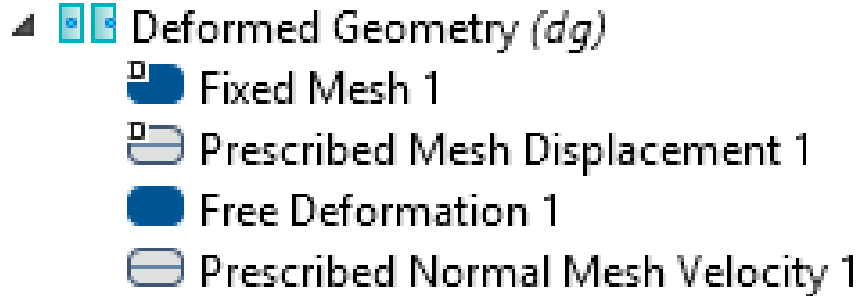


Figure 5.5 Sub tree of the Deformed Geometry Module

As for time, day was chosen as a unit and 0.2 day as a time step for 365 days.

To summarize how the model work, here's a simplification, after we implement the initial data and run the study, the (tds) module will calculate the first step, then the results will be passed to the (dg) module, which will calculate the corrosion interface deformation and redraw the model, then the model will be remeshed and submitted to the (tds) again and so on, until the time condition is met.

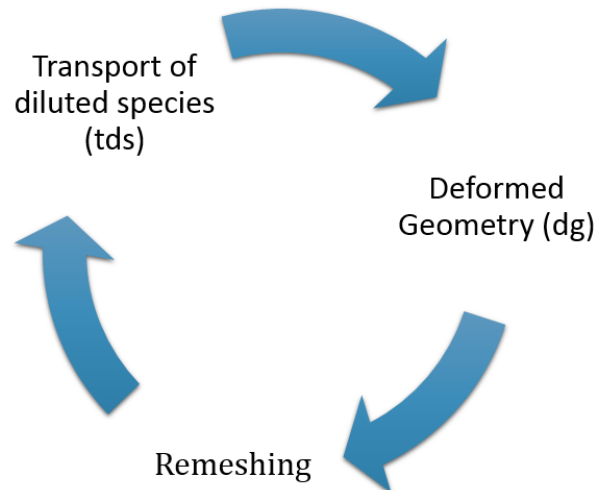


Figure 5.6 Representation of the three tasks done in each step

Further Analysis methods were used to compute the Mass loss, Magnesium dissolved in the medium and the generated hydrogen gas and hydroxide ions.

# CHAPTER 6

## Results

## 6. Results:

### 6.1. Model calibration:

The model is calibrated based on the experimental results found in I P Nanda et al [90], the simulation is run for pure Magnesium,  $Mg - 2Zn$ ,  $Mg - 4Zn$ ,  $Mg - 6Zn$  and  $Mg - 8Zn$ .

The Diffusion of the medium is set to  $3e - 13 m^2/s$  which was selected to best fit the experimental results as mentioned before. And  $C_{Mg}$  is set to be invariable inside the implant.

The initial  $C_{env}$  is set to be the average Magnesium in the human body fluid and is estimated to be  $8.5e - 4 mol/m^3$ .

Table 6.1 showcase the values of  $C_{Mg}$  to be implemented for each alloy:

**Table 6.1: Magnesium concentration and Young Modulus of alloys.**

Alloy	$Mg$	$Mg - 2Zn$	$Mg - 4Zn$	$Mg - 6Zn$	$Mg - 8Zn$
$C_{Mg} (mol/m^3)$	71507.92	7077.76	68647.60	67217.44	65787.28
$E_0 (GPa)$	37.5	35.94	29.93	48.66	41.55

### 6.2. Implant degradation:

The figures 6.1 to 6.5 shows degradation of the implant and the concentration of Mg ions in the corrosion environment at 0, 120, 240, 360 days after immersion,



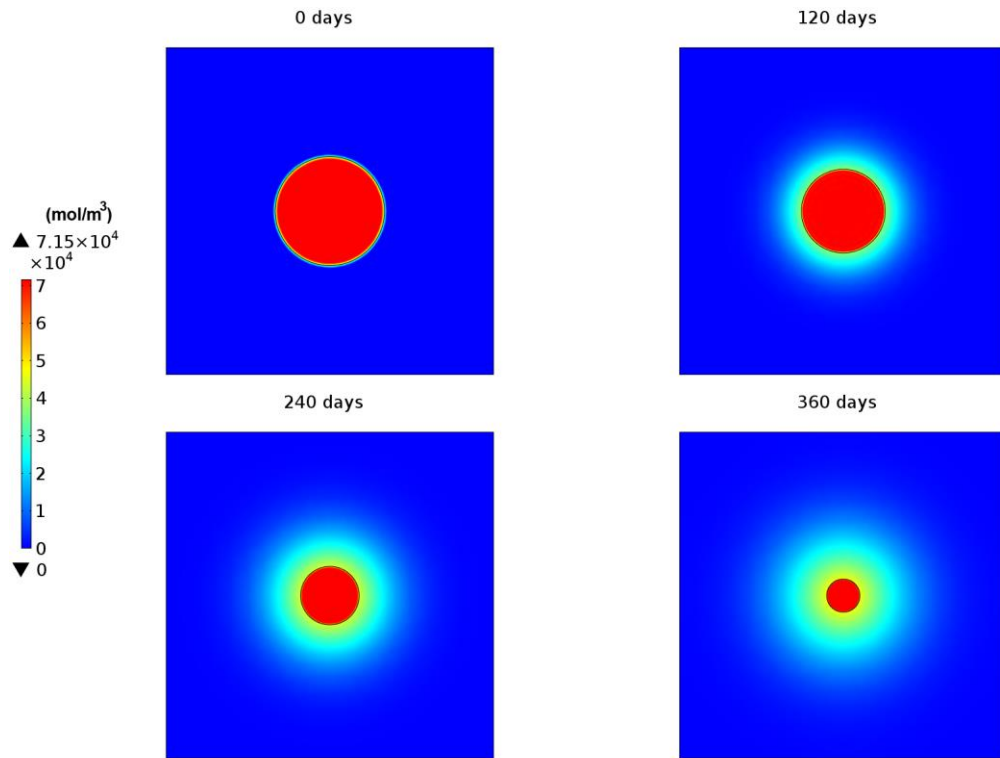


Figure 6.1 Contour plots of the implant degradation and corrosion environment concentration at 0, 120, 240 and 360 days after immersion of pure Mg.

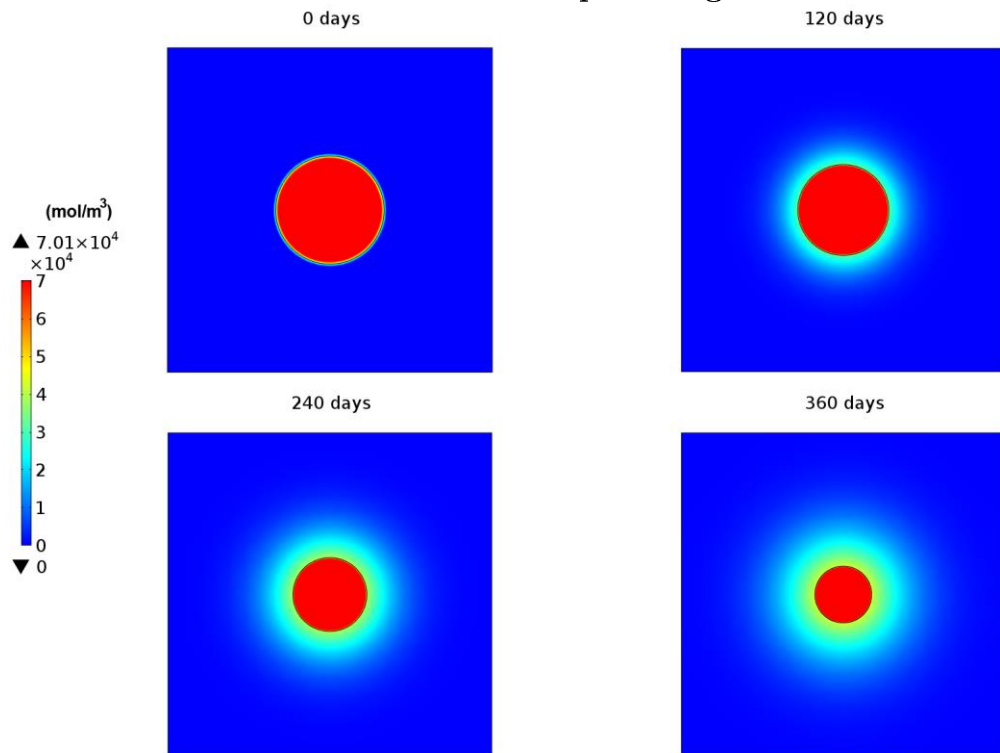


Figure 6.2 Contour plots of the implant degradation and corrosion environment concentration at 0, 120, 240 and 360 days after immersion of Mg-2Zn alloy.

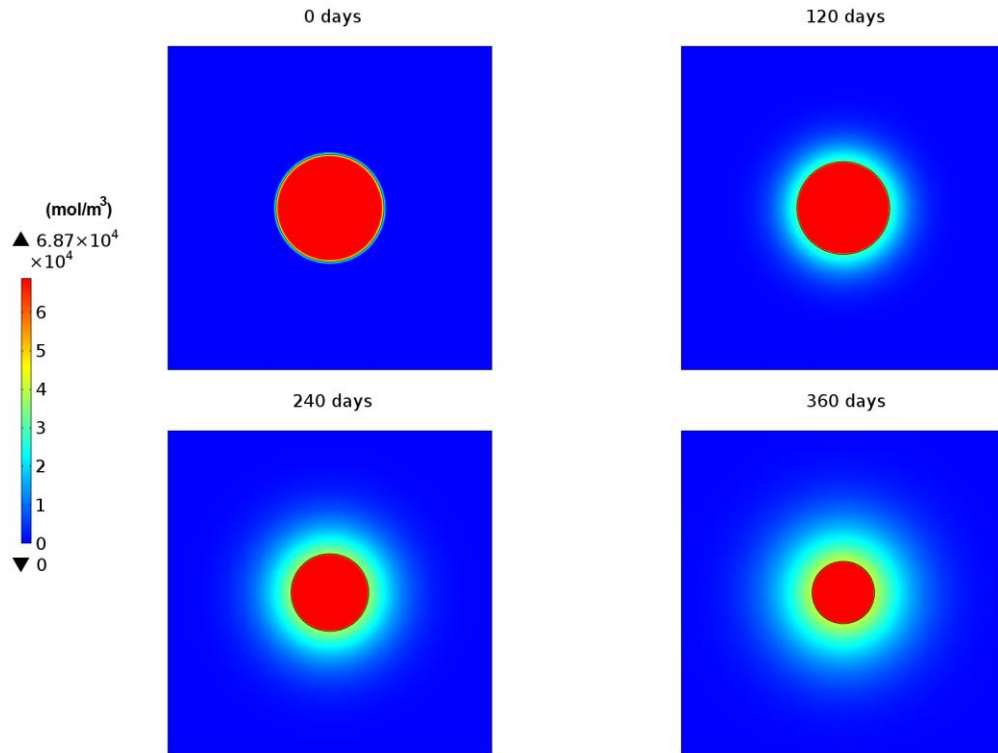


Figure 6.3 Contour plots of the implant degradation and corrosion environment concentration at 0, 120, 240 and 360 days after immersion of Mg-4Zn alloy.

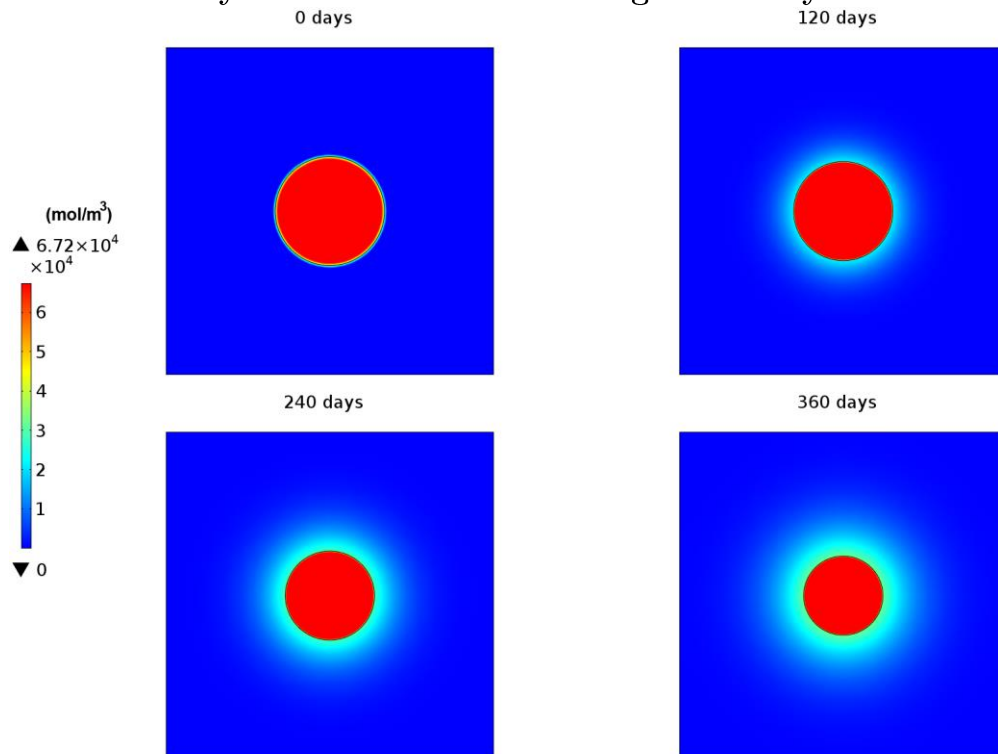


Figure 6.4 Contour plots of the implant degradation and corrosion environment concentration at 0, 120, 240 and 360 days after immersion of Mg-6Zn alloy.

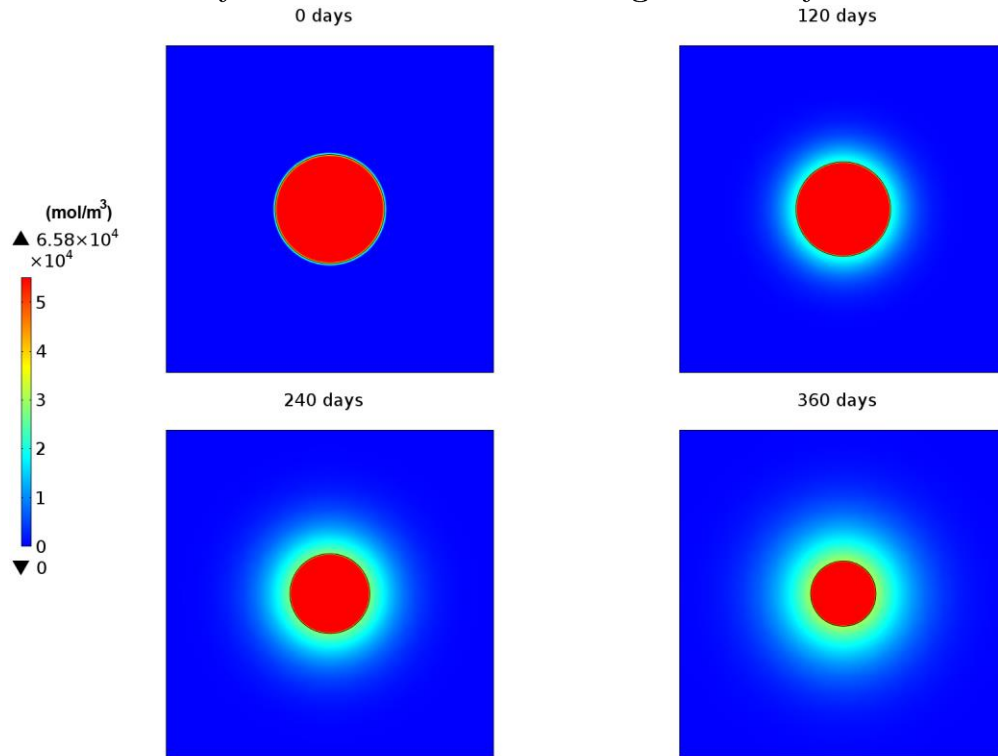


Figure 6.5 Contour plots of the implant degradation and corrosion environment concentration at 0, 120, 240 and 360 days after immersion of Mg-8Zn alloy.

In the figures 6.1 to 6.5 it is clear that the dimension reduces uniformly in cross section, when compared to experimental results of orthopedic implants in animals [91], the only difference is that the surface is rough in experiment which is due to the environment being more complicated, in a real biological environment the implant would experience many corrosion types, galvanic corrosion, pitting corrosion, stress corrosion and other forms and not only diffusion corrosion, but overall the profile is still the same as simulated results.

### 6.2.1. Mass loss:

Figure 6.6 represent the mass loss results of all the simulation, the profiles increase in an exponential way during the simulation we can fit the data obtained by the power formula:

$$\Delta V = At^B$$

To obtain a formula that describes the mass loss over time, where  $A$  and  $B$  are empirical parameters that are unique for each alloy.

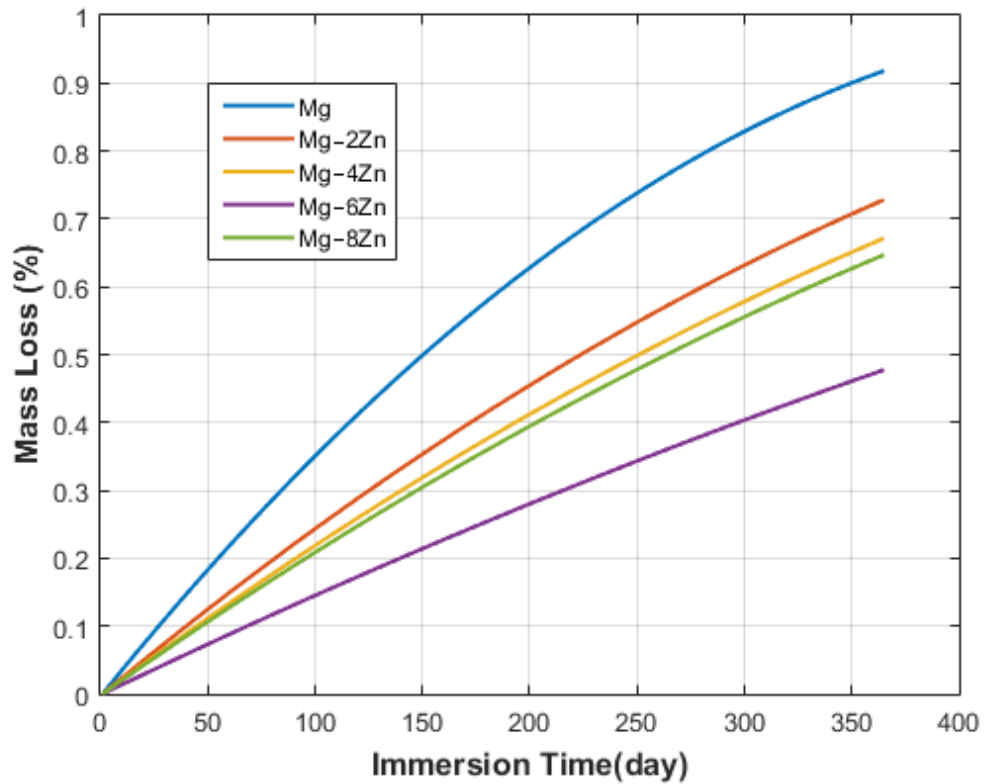


Figure 6.6: Evolution mass loss for simulated alloys

The empirical parameters were obtained using a Matlab fitting script:

Table 6.2: Empirical parameters of power function for simulated alloys

<i>Alloy</i>	<i>Mg</i>	<i>Mg – 2Zn</i>	<i>Mg – 4Zn</i>	<i>Mg – 6Zn</i>	<i>Mg – 8Zn</i>
<b><i>A</i></b>	0.01042	0.004818	0.003977	0.00209	0.0021
<b><i>B</i></b>	0.7672	0.8548	0.8729	0.9226	0.9226

And so, this formula can be used to predict the mass loss over a long time span without the computer simulation.

### 6.2.2. Magnesium ions diffused in the body:

Figure 6.7 represent the mass of Magnesium ions diffused in the biological body, to compute this data we estimated the length implant to be 410mm.

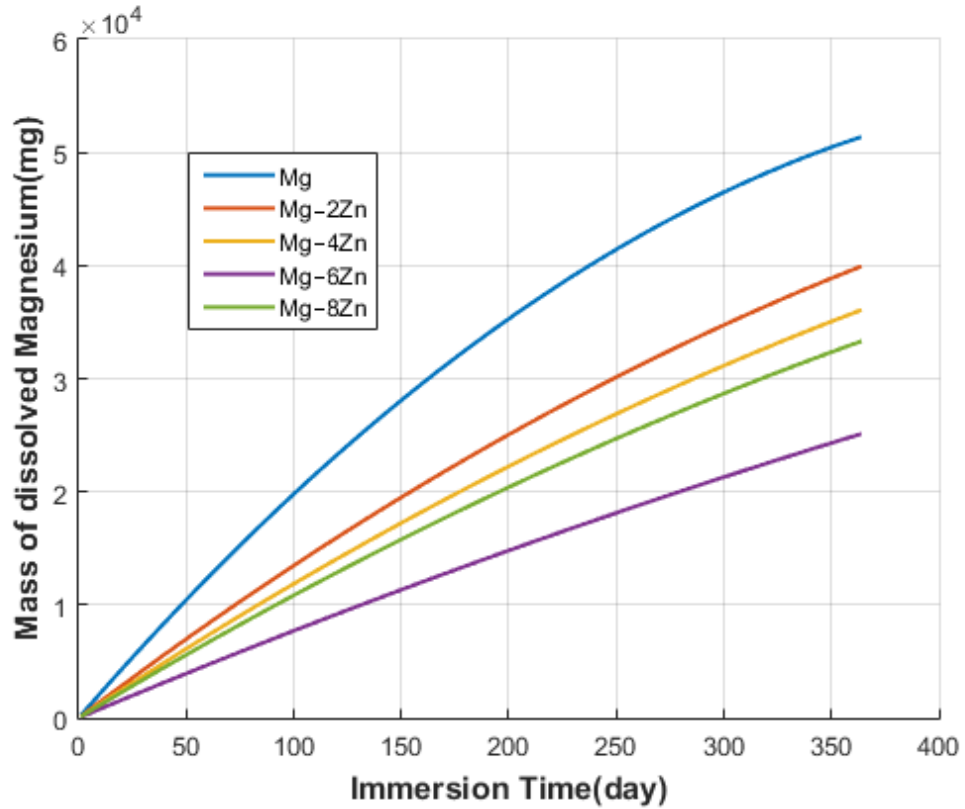
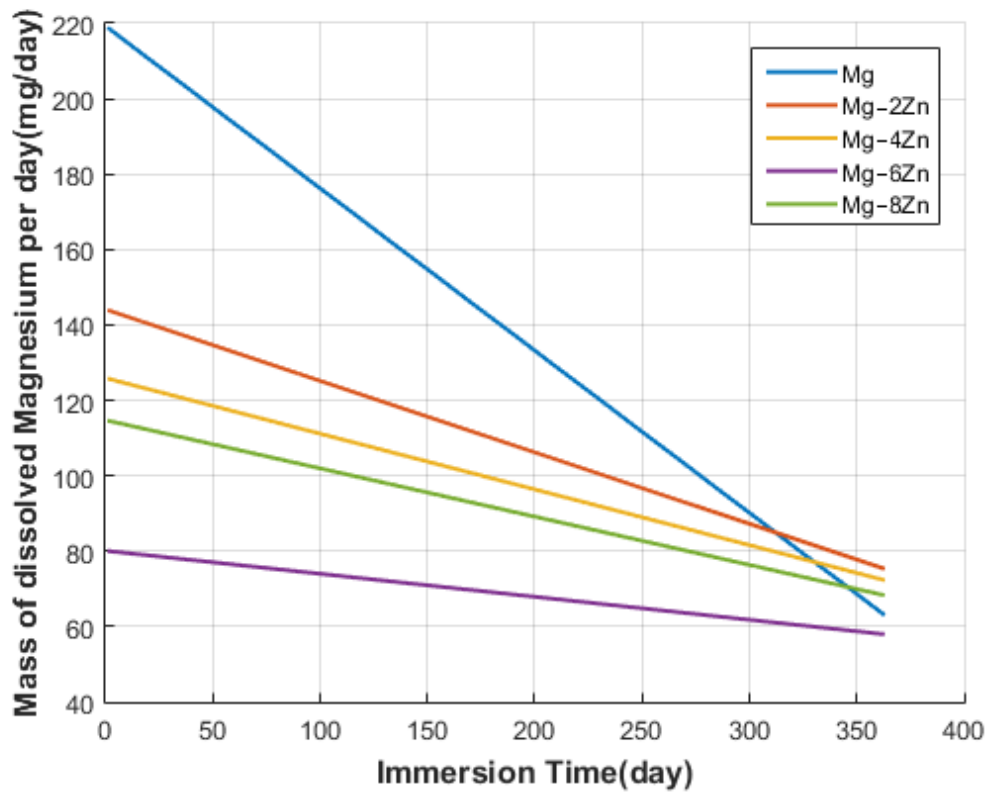


Figure 6.7: Evolution mass of dissolved Magnesium for simulated alloys

The curves in figure 6.7 can be fitted into power functions then derived to get curves of daily doses of diffused Magnesium ions:

Table 6.3: Empirical parameters of power function for simulated alloys

<i>Alloy</i>	<i>Mg</i>	<i>Mg – 2Zn</i>	<i>Mg – 4Zn</i>	<i>Mg – 6Zn</i>	<i>Mg – 8Zn</i>
<b>A</b>	604.2976	274.0673	221.7080	114.1516	195.9814
<b>B</b>	0.7614	0.8488	0.8669	0.9166	0.8741



**Figure 6.8: Evolution mass of dissolved Magnesium per day for simulated alloys**

We can see in figure 6.8 that amounts of Magnesium ions dissolved to the body vary depending on the alloys and its value is relative to the corrosion rate of the alloy, the data shown in figure 6.8 are promising, about 300-400 mg/day are required for the human body's metabolic activities [92], and all the alloys studied diffused an inferior amount of Mg ions to the previous amount. The dissolved Mg ions will be consumed by the body. Even if the amount exceeds the daily intake limit there's no worry because no side effects were ever found due to Mg ions overdose. The dissolution of a magnesium implant in the human body fluid is acceptable from a physiological point of view, and magnesium is the perfect choice when it comes to biocompatibility.

### 6.2.3. Hydrogen evolution:

As indicated in Equation (1), hydrogen gas is also a product of the magnesium corrosion, unlike Magnesium ions hydrogen can be harmful to the human body, in the case of an orthopedic implant the hydrogen bubbles will generate rapidly, which may delay the healing of the surgical region and death of tissues which will cause discomfort to the patients, figure 6.9 shows the evolution of generated hydrogen per day,

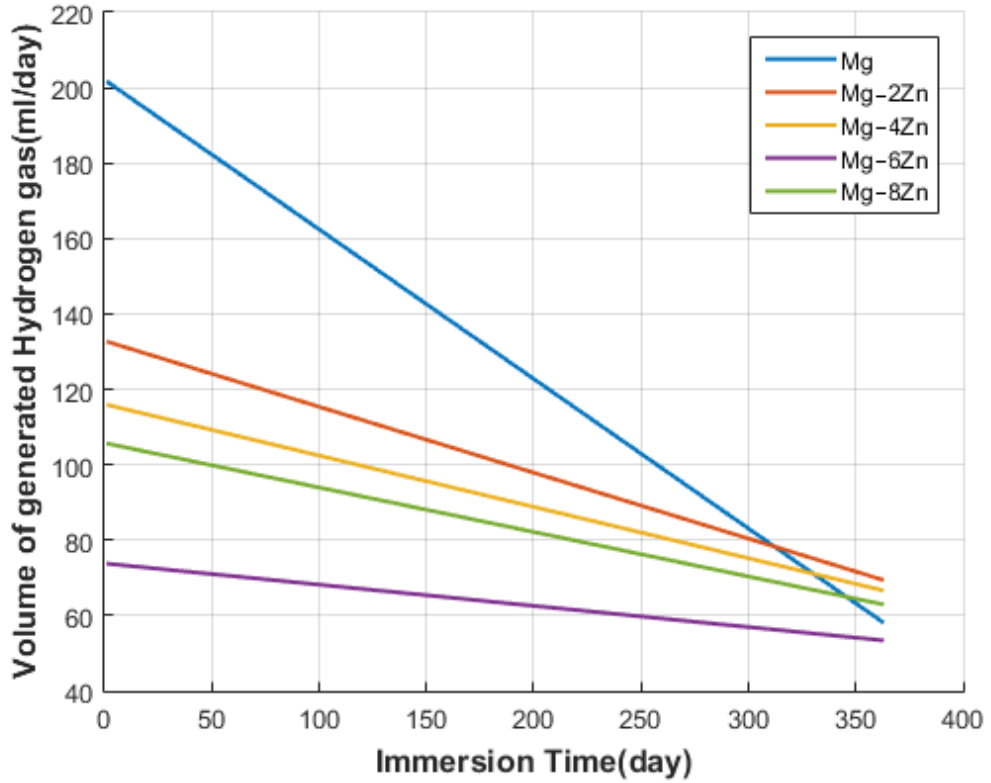


Figure 6.9: Evolution of Hydrogen gas volume for simulated alloys

All the studied alloys show high rate of hydrogen generation per day, Mg6Zn have the lowest rate by a large margin, although the results are for an implant of  $131.94 \text{ cm}^2$  surface area. Research found that human body do consume molecular hydrogen at a rate of  $0.7 \mu\text{mol} \cdot \text{min}^{-1} \cdot \text{m}^{-2} \text{BSA}$  [93], the equivalent of  $22.5792 \text{ ml} \cdot \text{day}^{-1} \cdot \text{m}^{-2} \text{BSA}$ , the average BSA of an adult human is  $1.7 \text{ m}^2$ , so if the hydrogen is distributed throughout the whole body a dose of  $38.38 \text{ ml} \cdot \text{day}^{-1}$ , Which set the maximum of the surface area of the implant to follow the equation:

$$S_{max} = \frac{38.38}{V_{H_2}}$$

Where  $V_{H_2}$  the generation rate of hydrogen per day, this result is an estimation and further research must be done before it can be validated.

#### 6.2.4. Evolution of Hydroxide ions:

Hydroxide ions are another product of Magnesium corrosions as the Equation (1) indicates, figure 6.10 present the doses of Hydroxide ions generated per day.

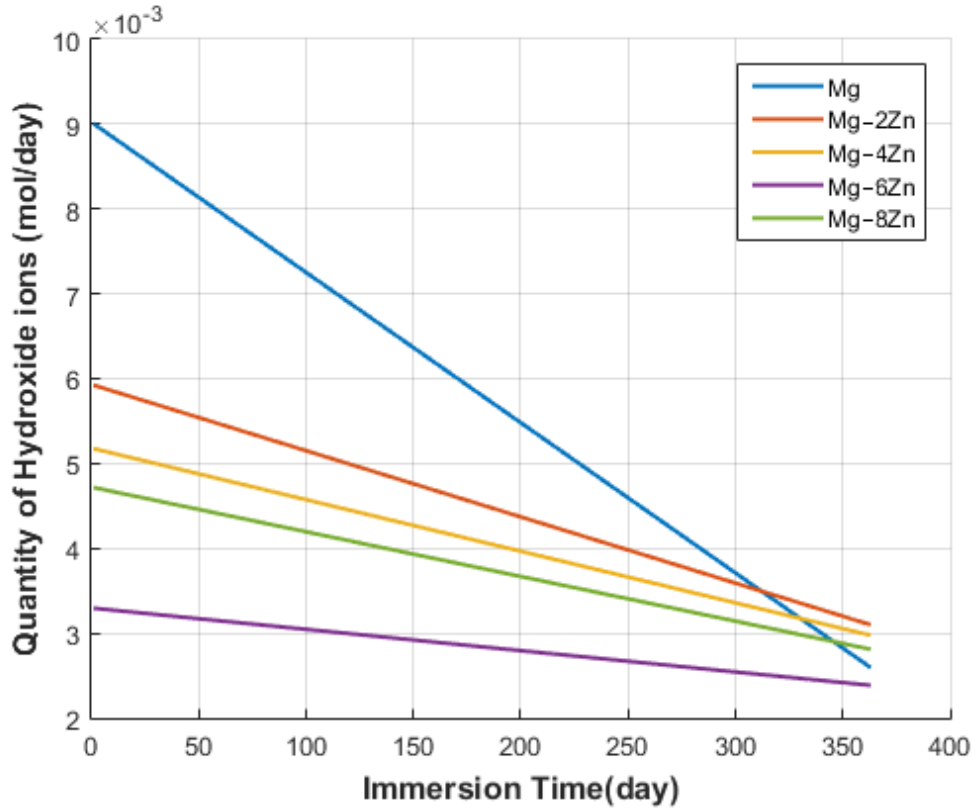


Figure 6.10: Evolution Hydroxide ions quantity for simulated alloys

The alkalization effect caused by corroding magnesium was found to increase the SBF pH value to over 9 in approximately 10 hours and finally to a relatively stable 10.5 value. This means that if a magnesium component is implanted in the human body, it will increase local pH value of body fluid, ear the magnesium implant. Clearly, body fluid alkalization can greatly affect the equilibrium of physiological reactions in the human body, which is not wanted at all. The curves in figure6.10 show high rates of hydroxide ions, which indicated that the use of these alloys will increase the local pH which may cause severe reaction in the human body.



### 6.2.5. Effective Young Modulus:

In the biological body bone will grow on the degraded area of the implant, thus we can estimate the effective Young modulus  $E_{eff}$  using the equation:

$$E_{eff} = E_b \cdot q + E_0(1 - q)$$

Where  $E_b$  is the Young modulus of the femur bone which is estimated to be  $18.7 \text{ GPa}$ ,  $E_0$  is Young modulus of the implants alloy, and  $q$  is the mass loss. The evolution of estimated effective Young's modulus for the studied alloys is presented in figure 6.11.

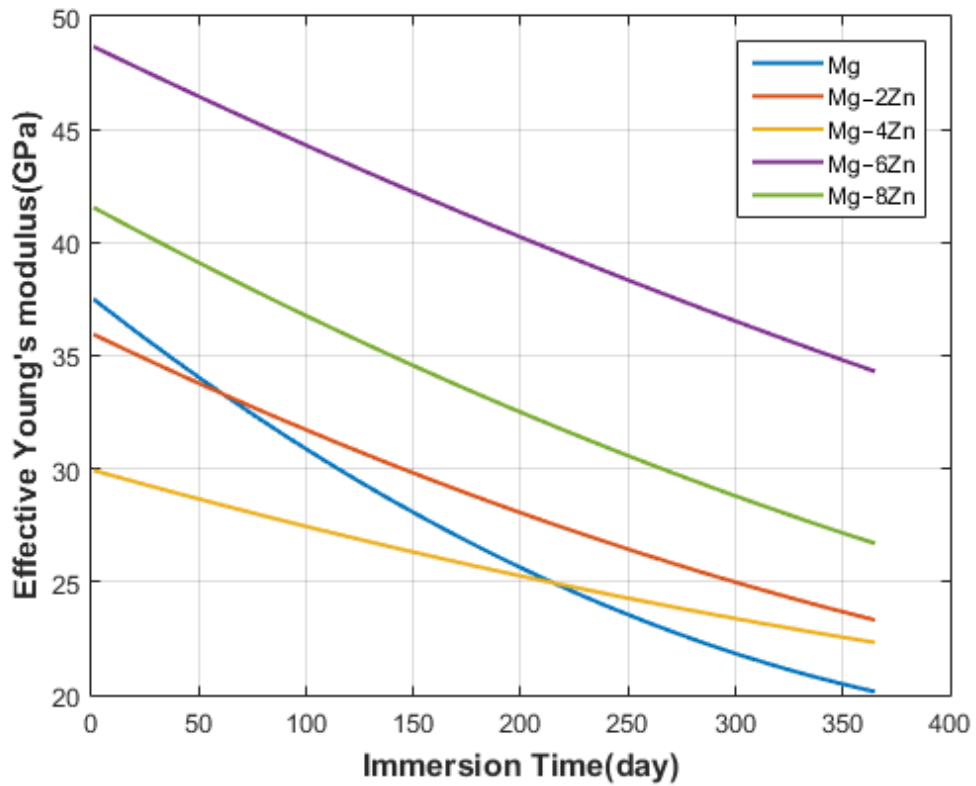


Figure 6.11: Evolution effective Young's modulus for simulated alloys

All the studied alloys displayed satisfactory mechanical proprieties, which allow the implants to support the bones during the healing period.

### 6.3. Possible solutions the encountered problems:

Rapid corrosion of Mg in SBF will lead to a great amount of dissolved  $Mg^{2+}$ , a large volume of hydrogen gas generated, and a remarkable increase in local pH value of body fluid in the human body. As demonstrated above, the hydrogen evolution and alkalization resulting from corrosion of Mg are the most critical obstacles in using magnesium as an implant material. A straightforward strategy to tackle these difficulties is to reduce the corrosion rate. A low corrosion rate of a magnesium implant means low rates of hydrogen evolution and OH-generation, which will allow the human body to gradually absorb or consume these corrosion by-products and to avoid formation of subcutaneous bubbles and alkalization of body fluid.

#### 6.3.1. Alloying elements:

Alloying can significantly slow down the corrosion rate of Mg in SBF. However, in practice, most alloying elements will be dissolved into the human body together with magnesium after a magnesium alloy degrades. This is unfavorable to the human body from a health point of view.

In addition, most heavy metal elements are poisonous to the human body. They should not be used as alloying elements. Therefore, the unfavorable alloying elements currently to a great extent limit the approach of alloying or using existing magnesium alloys.

#### 6.3.2. Surface treatment and coating:

Another approach of improving the corrosion resistance of Mg is surface treatment or coating. For example, anodizing is an important surface treatment for magnesium alloys, which can effectively slow down the corrosion rate of Mg and its alloys simply because:

- An anodized coating is hard compared with other conversion coating or fluoridated coating, and hence should be wear resistant in practice.
- An anodized coating is usually porous similar to the cancellous microstructure of a bone, which might be favorable to the growth of bone tissue

As the coating contains about 30 % Si and the coating is only about 4  $\mu m$  thick, if 1  $cm^2$  surface area is dissolved, then only about 2.7  $\mu g$  Si is dissolved into body fluid. Considering the high corrosion resistance of anodized Mg, a considerably long time will be required to dissolve the 2.7  $\mu g$  Si on a 1  $cm^2$  surface of Mg. Therefore, in practice only a trace

amount of Si can actually get into the human body. Research suggested that trace amount of Si is essential in mammals. In this sense, the anodized coating should be non-toxic to the human body. The most attractive feature of anodized coating is that it can offer very effective protection before the surgery region has healed. After that, it will break down to allow the implant to be dissolved gradually.

# General Conclusion

In conclusion this study proved that the degradation of Magnesium Zinc implants can be simulated using a diffusion-based Model, and acquired data were compatible with experimental results.

Functions with empirical parameters can be deduced from simulation data to help estimate the evolutions of the different corrosion products without the need of running the simulation.

Magnesium Zinc alloys show ideal mechanical proprieties and excellent biocompatibility, although the alloys are not ready to use directly due to problems of high hydrogen release and local alkalization of body fluid near the surgical region.

Many technologies exist or are in development that can remove the flaws of Magnesium alloys by reducing the corrosion rate.

Further experimental studies about other types of corrosion like galvanic corrosion, stress corrosion and pitting corrosion need to be done to improve the numerical model and its accuracy.

## References:

- [1] Draughn R. A., An Y. H., "Mechanical properties of bone," in Mechanical testing of bone and the bone-implant interface. CRC Press, 1999
- [2] W. Jee and S. Cowin, "Integrated Bone Tissue Physiology: Anatomy and Physiology," in Bone mechanics handbook - Second edition. CRC Press, 2001
- [3] Guo, X. E., Hu, Y. J., & Dinescu, A. T. (2020). Bone Structure and Function. Reference Module in Biomedical Sciences.
- [4] Richards AM, Coleman NW, Knight TA, Belkoff SM, and Mears SC (2010) Bone density and cortical thickness in normal, osteopenic, and osteoporotic sacra. Journal of Osteoporosis 2010.
- [5] Jones HH, Priest JD, Hayes WC, Tichenor CC, and Nagel DA (1977) Humeral hypertrophy in response to exercise. The Journal of Bone and Joint Surgery. American Volume 59: 204–208.
- [6] Chen H, Zhou X, Shoumura S, Emura S, and Bunai Y (2010) Age- and gender-dependent changes in three-dimensional microstructure of cortical and trabecular bone at the human femoral neck. Osteoporosis International 21: 627–636.
- [7] S. C. Cowin, A. E. Goodship, J. L. Cunningham, "Bone adaptation," in Bone Mechanics Handbook, Second Edition.: Taylor and Francis, 2001, ch. 5
- [8] B. Cummings, Bone fracture healing process, 2004, Pearson Education, Inc
- [9] W. R. Fordham, S. Redmond, A. Westerland, et al., "Silver as a bactericidal coating for biomedical implants," Surface & coatings technology, vol. 253, pp. 52-57, 2014
- [10] R. Marsell and T. A. Einhorn, "The biology of fracture healing," Injury, vol. 42, pp.551-555, 2011
- [11] Guo, X. E., Hu, Y. J., & Dinescu, A. T. (2020). Bone Structure and Function. Reference Module in Biomedical Sciences; 238-239
- [12] Cowin SC (2001) Bone Mechanics Handbook. Boca Raton, FL: CRC Press.

- [13] Mizrahi J, Silva MJ, Keaveny TM, Edwards WT, and Hayes WC (1993) Finite-element stress analysis of the normal and osteoporotic lumbar vertebral body. *Spine (Phila Pa 1976)* 18: 2088–2096
- [14] Rho JY, Ashman RB, and Turner CH (1993) Young’s modulus of trabecular and cortical bone material: Ultrasonic and microtensile measurements. *Journal of Biomechanics* 26: 111–119.
- [15] Characterization of Implantation’s Biomaterials Based on the Patient and Doctor Expectations: 3-4.
- [16] Edward Guo, Yizhong Jenny Hu, and A Teodora Dinescu, Bone Structure and Function ;Bioengineering Laboratory, Department of Biomedical Engineering, Columbia University, New York, NY, United States; 237-240
- [17] J. Park and R. S. Lakes, *Biomaterials: an introduction*. Springer Science & Business Media, 2007.
- [18] C. Ruff, B. Holt, and E. Trinkaus, “Who’s afraid of the big bad Wolff?: ‘Wolff’s law’ and bone functional adaptation,” *Am. J. Phys. Anthropol. Off. Publ. Am. Assoc. Phys. Anthropol.*, vol. 129, no. 4, pp. 484–498, 2006.
- [19] Y. Zheng, X. Gu, and F. Witte, “Biodegradable metals,” *Mater. Sci. Eng. R Rep.*, vol. 77, pp. 1–34, 2014.
- [20] J. C. Middleton and A. J. Tipton, “Synthetic biodegradable polymers as orthopedic devices,” *Biomaterials*, vol. 21, no. 23, pp. 2335–2346, 2000.
- [21] M. S. Taljanovic, M. D. Jones, J. T. Ruth, J. B. Benjamin, J. E. Sheppard, and T. B. Hunter, “Fracture fixation,” *Radiographics*, vol. 23, no. 6, pp. 1569–1590, 2003.
- [22] Bose S, Ke D, Sahasrabudhe H, et al., 2017, Additive manufacturing of biomaterials. *Prog Mater Sci*, 93:1-310
- [23] Parthasarathy J, 2014, 3D modeling, custom implants and its future perspectives in craniofacial surgery. *Ann Maxillofac Surg*, 4(1): 9
- [24] Jardini A L, Larosa M A, Bernardes L F, et al., 2014, Customised titanium implant fabricated in additive manufacturing for craniomaxillofacial surgery. *Virtual Phys Prototyp*, 9(2): 115–125
- [25] Yan R, Luo D, Huang H, et al., 2018, Electron beam melting in the fabrication of three-dimensional mesh titanium mandibular prosthesis scaffold. *Sci Rep*, 8(1): 750

- [26] F. Lux, J. Schuster, and R. Zeisler, “A mechanistic model for the metabolism of corrosion products and of biological trace elements in metallosis tissue based on results obtained by activation analysis,” *J. Radioanal. Nucl. Chem.*, vol. 32, no. 1, 2007.
- [27] E. J. Heffernan, M. M. Hayes, F. O. Alkubaidan, P. W. Clarkson, and P. L. Munk, “Aggressive angiomyxoma of the thigh,” *Skeletal Radiol.*, vol. 37, no. 7, pp. 673–678, Jul. 2008.
- [28] A. Oriňák *et al.*, “Sintered metallic foams for biodegradable bone replacement materials,” *J. Porous Mater.*, vol. 21, no. 2, pp. 131–140, 2014.
- [29] N. H. Munro and K. M. McGrath, “Advances in techniques and technologies for bone implants,” *Bioinspired Biomim. Nanobiomaterials*, vol. 4, no. 1, pp. 26–36, 2015.
- [30] F. Witte *et al.*, “In vivo corrosion and corrosion protection of magnesium alloy LAE442,” *Acta Biomater.*, vol. 6, no. 5, pp. 1792–1799, 2010.
- [31] J. Reifenrath, D. Bormann, and A. Meyer-Lindenberg, “Magnesium alloys as promising degradable implant materials in orthopaedic research,” *Magnes. Alloy. Surf. Treat.*, pp. 93–108, 2011.
- [32] K. Rezwan, Q. Chen, J. J. Blaker, and A. R. Boccaccini, “Biodegradable and bioactive porous polymer/inorganic composite scaffolds for bone tissue engineering,” *Biomaterials*, vol. 27, no. 18, pp. 3413–3431, 2006.
- [33] E. Wintermantel and S.-W. Ha, *Medizintechnik: Life Science Engineering*. Springer Science & Business Media, 2009.
- [34] F. Horste and B. Mordike, “Magnesium technology, metallurgy, design data, application [M],” 2006.
- [35] R. Huiskes, H. Weinans, and B. Van Rietbergen, “The relationship between stress shielding and bone resorption around total hip stems and the effects of flexible materials,” *Clin. Orthop.*, pp. 124–134, 1992.
- [36] H. E. Friedrich and B. L. Mordike, *Magnesium Technology: Metallurgy, Design Data, Applications*. Berlin, Heidelberg: Springer-Verlag Berlin Heidelberg, 2006.
- [37] A. Nayeb-Hashemi, “Phase diagrams of binary magnesium alloys,” *ASM Int. Met. Park Ohio 44073 USA 1988 370*, 1988.



- [38] G. Neite, K. Kubota, K. Higashi, and F. Hehmann, "In RW Cahn, P. Haasen, and EJ Kramer," *Mater. Sci. Technol.*, vol. 8, 2005.
- [39] K. U. Kainer and B. L. Mordike, *Magnesium alloys and their applications*. Wiley-VCH Weinheim, 2000.
- [40] M. Gupta and S. N. M. Ling, *Magnesium, magnesium alloys, and magnesium composites*. John Wiley & Sons, 2011.
- [41] E. D. McBRIDE, "ABSORBABLE METAL IN BONE SURGERY: A FURTHER REPORT ON THE USE OF MAGNESIUM ALLOYS," *J. Am. Med. Assoc.*, vol. 111, no. 27, p. 2464, Dec. 1938.
- [42] M. P. Staiger, A. M. Pietak, J. Huadmai, and G. Dias, "Magnesium and its alloys as orthopedic biomaterials: a review," *Biomaterials*, vol. 27, no. 9, pp. 1728–1734, 2006.
- [43] Y. Song, D. Shan, R. Chen, F. Zhang, and E.-H. Han, "Biodegradable behaviors of AZ31 magnesium alloy in simulated body fluid," *Mater. Sci. Eng. C*, vol. 29, no. 3, pp. 1039–1045, 2009.
- [44] Y. Zheng, *Magnesium alloys as degradable biomaterials*. CRC Press, 2015.
- [45] K. Hewitt and T. Wall, *The zinc industry*. Elsevier, 2000.
- [46] G. Song, A. Atrens, *Advanced Engineering Materials* 1 (1999) 11–33.
- [47] G.L. Song, A. Atrens, *Advanced Engineering Materials* 5 (2003) 837]
- [48] F. Witte, J. Fischer, J. Nellesen, H.A. Crostack, V. Kaese, A. Pisch, F. Beckmann, H. Windhagen, *Biomaterials* 27 (2006) 1013–1018
- [49] Virtanen, S. *Corrosion of biomedical implant materials*. *Corros. Rev.* 2008, 26, 147–171
- [50] Eliaz, N.; Gileadi, E. *Physical Electrochemistry: Fundamentals, Techniques, and Applications*, 2nd ed.; Wiley-VCH: Weinheim, Germany, 2019;
- [51] *Magnesium for biomedical applications as degradable implants : thermomechanical processing and surface functionalization of a Mg-Ca alloy* Olivier Jay , 51-52
- [52] G. L. Song and A. Atrens, "Corrosion mechanisms of magnesium alloys," *Advanced engineering materials*, vol. 1, pp. 11-33, 1999

- [53] E. Gali, "Part 1 - Electrochemical fundamentals and active-passive corrosion behaviors," in *Corrosion Resistance of Aluminum and Magnesium Alloys: Understanding, Performance, and Testing.*: Wiley, 2010
- [54] Polmear I., "Magnesium alloys and applications," *Materials Science and Technology*, vol. 10, pp. 1-16, 1994.) ( E. Gali, "Part 1 - Electrochemical fundamentals and active-passive corrosion behaviors," in *Corrosion Resistance of Aluminum and Magnesium Alloys: Understanding, Performance, and Testing.*: Wiley, 2010
- [55] P. Kurze, "Corrosion and Corrosion Protection of Magnesium," in *Magnesium - Alloys and Technologies.*: Wiley-VCH, 2004, ch. 13
- [56] Song G., Atrens A., John D.S., Wu X., Nairn J. The anodic dissolution of magnesium in chloride and sulphate solutions. *Corros. Sci.* 1997;39:1981–2004.
- [57] Poinern G.E.J., Brundavanam S., Fawcett D. Biomedical Magnesium Alloys: A Review of Material Properties, Surface Modifications and Potential as a Biodegradable Orthopaedic Implant. *Am. J. Biomed. Eng.* 2012;2:218–240.
- [58] Song G. Control of biodegradation of biocompatible magnesium alloys. *Corros. Sci.* 2007;49:1696–1701.
- [59] In vivo corrosion of four magnesium alloys and the associated bone response. Witte F, Kaese V, Haferkamp H, Switzer E, Meyer-Lindenberg A, Wirth CJ, Windhagen H *Biomaterials.* 2005 Jun; 26(17):3557-63.
- [60] J.-L. Crolet and G. Béranger, "Corrosion en milieu aqueux des métaux et alliages," in *Corrosion et vieillissement: phénomènes et mécanismes.* Techniques de l'Ingenieur, 1998
- [61] G. L. Song and A. Atrens, "Corrosion mechanisms of magnesium alloys," *Advanced engineering materials*, vol. 1, pp. 11-33, 1999
- [62] R.-C. Zeng, J. Zhang, W.-J. Huang, et al., "Review of studies on corrosion of magnesium alloys," *Transactions of nonferrous metals society of China*, vol. 16, pp. 763-771, 2006
- [63] G. L. Song and A. Atrens, "Corrosion mechanisms of magnesium alloys," *Advanced engineering materials*, vol. 1, pp. 11-33, 1999

- [64] E. Gali, "Part 3 - Properties, use, and performance of magnesium and its alloys," in *Corrosion Resistance of Aluminum and Magnesium Alloys Understanding, Performance.*: Wiley, 2010b
- [65] R.-C. Zeng, J. Zhang, W.-J. Huang, et al., "Review of studies on corrosion of magnesium alloys," *Transactions of nonferrous metals society of China*, vol. 16, pp.763-771, 2006
- [66] J. Li, Y. Song, S. Zhang et al., "In vitro responses of human bone marrow stromal cells to a fluoridated hydroxyapatite coated biodegradable Mg-Zn alloy," *Biomaterials*, vol. 31, no. 22, pp. 5782–5788, 2010.
- [67] S. Cai, T. Lei, N. Li, and F. Feng, "Effects of Zn on microstructure, mechanical properties and corrosion behavior of Mg-Zn alloys," *Materials Science and Engineering C: Materials for Biological Applications*, vol. 32, no. 8, pp. 2570–2577, 2012.
- [68] H. Wang and Z. Shi, "In vitro biodegradation behavior of magnesium and magnesium alloy," *Journal of Biomedical Materials Research Part B: Applied Biomaterials*, vol. 98, no. 2, pp. 203–209, 2011.
- [69] J. E. Gray-Munro, C. Seguin, and M. Strong, "Influence of surface modification on the in vitro corrosion rate of magnesium alloy AZ31," *Journal of Biomedical Materials Research Part A*, vol. 91, no. 1, pp. 221–230, 2009.
- [70] A. A. Ghoneim, A. M. Fekry, and M. A. Ameer, "Electrochemical behavior of magnesium alloys as biodegradable materials in Hank's solution," *Electrochimica Acta*, vol. 55, no. 20, pp. 6028–6035, 2010.
- [71] F. Witte, J. Fischer, J. Nellesen et al., "In vitro and in vivo corrosion measurements of magnesium alloys," *Biomaterials*, vol. 27, no. 7, pp. 1013–1018, 2006.
- [72] M. Shahzad and L. Wagner, "The role of Zr-rich cores in strength differential effect in an extruded Mg-Zn-Zr alloy," *Journal of Alloys and Compounds*, vol. 486, no. 1-2, pp. 103–108, 2009.
- [73] D. Hong, P. Saha, D.-T. Chou et al., "In vitro degradation and cytotoxicity response of Mg-4% Zn-0.5% Zr (ZK40) alloy as a potential biodegradable material," *Acta Biomaterialia*, vol. 9, no. 10, pp. 8534–8547, 2013.

- [74] Kirkland N.T., Lespagnol J., Birbilis N., Staiger M.P. A survey of bio-corrosion rates of magnesium alloys. *Corros. Sci.* 2010;52:287–291.
- [75] Xin Y., Liu C., Zhang X., Tang G., Tian X., Chu P.K. Corrosion behavior of biomedical AZ91 magnesium alloy in simulated body fluids. *J. Mater. Res.* 2007;22:2004–2011.
- [76] Abe Y., Kokubo T., Yamamuro T. Apatite coating on ceramics, metals and polymers utilizing a biological process. *J. Mater. Sci. Mater. Med.* 1990;1:233–238.
- [77] Krasner P, Person P *J Am Dent Assoc.* 1992 Nov; 123(11):80-8
- [78] On the in vitro and in vivo degradation performance and biological response of new biodegradable Mg-Y-Zn alloys. Hänzi AC, Gerber I, Schinhammer M, Löffler JF, Uggowitzer PJ *Acta Biomater.* 2010 May; 6(5):1824-33
- [79] Inorganic plasma with physiological CO<sub>2</sub>/HCO<sub>3</sub><sup>-</sup> buffer. Marques PA, Magalhães MC, Correia RN *Biomaterials.* 2003 Apr; 24(9):1541-8
- [80] Song G. Control of biodegradation of biocompatible magnesium alloys. *Corros. Sci.* 2007;49:1696–1701.
- [81] William D.F., William R.L., Ratner B.D., Hoffman A.S., Schoen F.J., Lemons J.E. *Biomaterials Science*. 2nd ed. Elsevier; San Diego, CA, USA: 2004
- [82] Yamamoto A., Hiromoto S. Effect of inorganic salts, amino acids and proteins on the degradation of pure magnesium in vitro. *Mater. Sci. Eng. C.* 2009;29:1559–1568.
- [83] Abe Y., Kokubo T., Yamamuro T. Apatite coating on ceramics, metals and polymers utilizing a biological process. *J. Mater. Sci. Mater. Med.* 1990;1:233–238.
- [84] Song G.L., Xu Z. 5—Surface processing and alloying to improve the corrosion resistance of magnesium (Mg) alloys. In: Song G.-L., editor. *Corrosion Prevention of Magnesium Alloys*. Woodhead Publishing; Cambridge, UK: 2013. pp. 110–134
- [85] M. C. Turhan, R. Lynch, M. S. Killian, and S. Virtanen, “Effect of acidic etching and fluoride treatment on corrosion performance in Mg alloy AZ91D (MgAlZn),” *Electrochimica Acta*, vol. 55, no. 1, pp. 250–257, 2009.

- [86] J. E. Gray-Munro, C. Seguin, and M. Strong, “Influence of surface modification on the in vitro corrosion rate of magnesium alloy AZ31,” *Journal of Biomedical Materials Research Part A*, vol. 91, no. 1, pp. 221–230, 2009.
- [87] M. A. Melia, D. C. Florian, F. W. Steuer et al., “Investigation of critical processing parameters for laser surface processing of AZ31B-H24,” *Surface and Coatings Technology*, vol. 325, pp. 157–165, 2017.
- [88] A. C. W. Noorakma, H. Zuhailawati, V. Aishvarya, and B. K. Dhindaw, “Hydroxyapatite-coated magnesium-based biodegradable alloy: Cold spray deposition and simulated body fluid studies,” *Journal of Materials Engineering and Performance*, vol. 22, no. 10, pp. 2997–3004, 2013.
- [89] K. Krabbenhøft and J. Krabbenhøft, “Application of the Poisson Nernst–Planck equations to the migration test,” *Cement and Concrete Research*, vol. 38, no. 1, pp. 77–88, 2008.
- [90] I. P. Nanda, M. H. Hassim, M. H. Idris, M. H. Jahare, S. S. Abdulmalik, and A. Arafat, “Mechanical and degradation properties of zinc adopted magnesium alloys for biomedical application,” *IOP Conference Series: Materials Science and Engineering*, vol. 602, p. 012094, Sep. 2019,
- [91] Z. Shen et al., “Predicting the degradation behavior of magnesium alloys with a diffusion-based theoretical model and in vitro corrosion testing,” *Journal of Materials Science & Technology*, vol. 35, no. 7, pp. 1393–1402, 2019.
- [92] *Dietary Reference Intakes for Calcium, Phosphorus, Magnesium, Vitamin D, and Fluoride*. Washington, D.C.: National Academies Press, 1997, p. 5776.
- [93] A. Shimouchi, K. Nose, T. Mizukami, D.-C. Che, and M. Shirai, “Molecular hydrogen consumption in the human body during the inhalation of hydrogen gas,” in *Oxygen Transport to Tissue XXXV*, Springer, 2013, pp. 315–321.